



## Seasonal climatology of wind-driven circulation on the New Jersey Shelf

D. Gong,<sup>1</sup> J. T. Kohut,<sup>1</sup> and S. M. Glenn<sup>1</sup>

Received 15 May 2009; revised 24 September 2009; accepted 2 October 2009; published 3 April 2010.

[1] The spatial structure of the mean and seasonal surface circulation in the central region of the Mid-Atlantic Bight (New Jersey Shelf) are characterized using 6 years of CODAR long-range HF radar data (2002–2007). The mean surface flow over the New Jersey Shelf is 2–12 cm/s down shelf and offshore to the south. The detided root-mean-square (RMS) velocity variability ranges from 11 to 20 cm/s. The variability is on the order of the mean current offshore and several times that of the mean current nearshore. The Hudson Shelf Valley and the shelf break act as dynamical boundaries that define the New Jersey Shelf. The surface flow on the New Jersey Shelf depends on topography, seasonal stratification, and wind forcing. The flow is in the approximate direction of the wind during the unstratified season and more to the right of the wind during the stratified season. During the stratified summer season, the dominant along-shore upwelling favorable winds from the SW drive cross-shelf offshore flow. During the unstratified/well-mixed winter season, the dominant cross-shore NW winds drive cross-shelf offshore flows. During the transition seasons of spring and autumn, along-shore NE winds, often associated with storm events, drive energetic down-shelf, along-shelf flows. The surface transport pathways are either cross-shelf dominated during summer and winter or along-shelf dominated during the transition seasons. The residence time of surface Lagrangian drifters on the New Jersey Shelf ranged from 1 to 7 weeks with summer and autumn showing faster transport than winter and spring.

**Citation:** Gong, D., J. T. Kohut, and S. M. Glenn (2010), Seasonal climatology of wind-driven circulation on the New Jersey Shelf, *J. Geophys. Res.*, 115, C04006, doi:10.1029/2009JC005520.

### 1. Introduction

[2] The Middle Atlantic Bight (MAB), a shallow and wide continental shelf located off the east coast of the United States, is bounded by Cape Cod to the northeast and Cape Hatteras to the southwest (Figure 1). It is a highly productive shelf that exhibits strong seasonal cycles in both physical and biological processes [Bigelow, 1933; Bigelow and Sears, 1935; Beardsley and Boicourt, 1981; Yoder *et al.*, 2002]. Several major urban estuaries such as the Connecticut River, the Hudson River, the Delaware River and the Susquahanna River discharge into the bays and sounds connected to the MAB, delivering fresh and nutrient rich water onto the shelf. Transport of nutrients and organic material can determine the timing and distribution of shelf primary production and the subsequent response in the higher trophic levels [Yoder *et al.*, 2002; Schofield *et al.*, 2008]. An important objective of recent research projects is to characterize and quantify the cross-shelf exchange mechanisms and transport pathways on the

MAB [Biscaye *et al.*, 1994; Castelao *et al.*, 2008a; Chant *et al.*, 2008; Zhang *et al.*, 2009]. This transport is critical to the understanding of shelf marine ecosystem dynamics. The dynamics of shelf circulation are governed by the combined interactive forcing of many factors such as stratification [Lentz, 2001; Flagg *et al.*, 2002; Castelao *et al.*, 2008b], winds [Allen, 1980; Beardsley *et al.*, 1985; Lentz, 2001; Whitney and Garvine, 2005], storms [Keen and Glenn, 1995; Kohut *et al.*, 2006a; Glenn *et al.*, 2008], river discharge [Fong and Geyer, 2001; Byoung-Ju and Wilkin, 2007; Chant *et al.*, 2008], topography [Harris *et al.*, 2003; Zhang *et al.*, 2009], bottom boundary layers [Gawarkiewicz and Chapman, 1992; Chapman and Lentz, 1994; Keen and Glenn, 1994; Garvine, 2004], upstream forcing [Mountain, 2003], and offshore forcing [Gawarkiewicz *et al.*, 1996; Linder and Gawarkiewicz, 1998; Churchill *et al.*, 2003; Lentz, 2003]. The seasonal variability of the dominant processes impacts the coupled seasonal biological response. The set of forcing factors driving the dynamics of the midshelf or the outer shelf is often different from that of the inner shelf. Whereas buoyancy forcing and bottom friction play major roles in the inner shelf dynamics, winds and changing stratification are the major drivers of the dynamics at the mid to outer shelf. In this study, a 6 year time series of HF Radar surface current data from Rutgers University Coastal Ocean

<sup>1</sup>Institute of Marine and Coastal Sciences, Rutgers-State University of New Jersey, New Brunswick, New Jersey, USA.

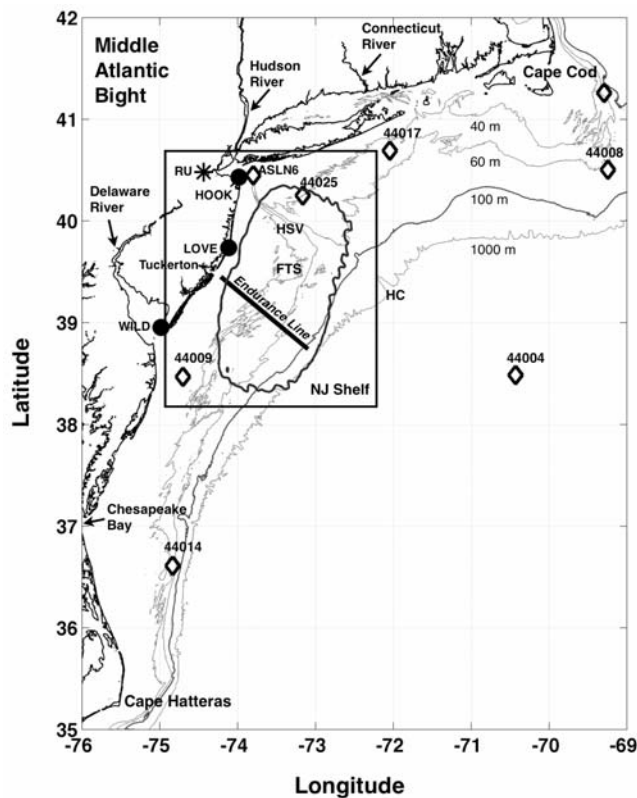


**Figure 1.** Middle Atlantic Bight from Cape Hatteras up to Cape Cod. The 40, 60, 100, and 1000 m isobaths are marked. HSV, Hudson Shelf Valley; HC, Hudson Canyon; FTS, Fortune Tiger Shore; RU, Rutgers University; HOOK, Sandy Hook CODAR site; LOVE, Loveladies CODAR site; WILD, Wildwood CODAR site. The 50% CODAR coverage area for the New Jersey Shelf is outlined. NOAA NDBC buoys are marked as diamonds and are labeled.

Observation Lab [Glenn and Schofield, 2009] is used to characterize the effect of topography, seasonal stratification and wind forcing on the surface subtidal circulation and transport at the mid to outer portion of the New Jersey Shelf. In particular, the surface flows during the transition seasons of spring and autumn are characterized and compared with the stratified summer as well as the unstratified winter. A seasonal climatology of the wind-driven surface current response is constructed and the seasonal transport patterns and residence times are examined.

[3] This paper is structured as follows. In section 2, we review the relevant physical processes affecting circulation and transport on the New Jersey Shelf. In section 3, we describe the 6 year Rutgers HF Radar and National Oceanic and Atmospheric Administration (NOAA) National Data Buoy Center (NDBC) weather buoy data set used in this analysis. In section 4.1, we characterize the mean and the subtidal variability of surface flow. In section 4.2, we characterize the low-wind background flow and effect of topographic features such as the Hudson Shelf Valley (HSV) and the Fortune/Tiger Shore (FTS). In section 4.3, we discuss the effect of seasonal variability in stratification and wind on the mean flow over seasonal time scales. In

section 4.4, we discuss the response of surface flow to seasonal wind forcing. In section 4.5, we present the seasonal climatology of the wind-current correlation. In section 4.7, we calculate the seasonal cross-shelf transport pathways and shelf residence time. Finally in section 4.6, we explore the interannual variability of the current response to changes in seasonal forcing. The results are discussed in section 5 and summarized in section 6.

## 2. Background

### 2.1. Mean Flow and Upstream Sources

[4] Studies using geochemical tracers have shown that the upstream source of MAB shelf water originates from southern Greenland with a volume flux of 4–5 Sverdrups [Chapman and Beardsley, 1989]. Most of this water exits the shelf as it travels down shelf. By the time the coastal current enters the MAB, the mean volume flux drops to approximately 0.4 Sverdrups [Beardsley *et al.*, 1985]. Historically, the depth-averaged mean flow on the MAB is shown to be 3–7 cm/s down shelf toward the southeast based on current meter moorings [Beardsley and Boicourt, 1981]. A recent study using an expanded data set of current meter measurements shows that the mean depth-averaged along-shore flow on the shelf is constant along-isobath and is linearly correlated with the depths of the isobaths, decreasing toward shore [Lentz, 2008a]. This along-shelf flow has been largely attributed to a basin-scale along-shelf pressure gradient [Beardsley and Winant, 1979; Lentz, 2008a]. A climatological study of MAB hydrography found that shelf water volume (characterized by salinity <34) on the New Jersey Shelf varied seasonally with a magnitude on the order of the mean shelf water volume [Mountain, 2003]. Variability about the mean shelf flow is significant on various temporal and spatial scales ranging from tidal to interannual and from internal Rossby radius to shelf-wide length scales [Beardsley *et al.*, 1985; Lentz, 2008b; Dzwonkowski *et al.*, 2009a].

### 2.2. Topography

[5] Topographic variations on the shelf-wide scale can play an important role on along-shelf and cross-shelf transport. The Hudson Shelf Valley (HSV) is the only remaining submarine shelf valley that cuts perpendicularly across the entire width of the MAB shelf. The Fortune/Tiger Shore (FTS) [Knebel and Spiker, 1977; Thielier *et al.*, 2007], an ancient shoreline to the south of the HSV, is outlined by the 40 m isobath (Figure 1). The steep topography between the 40 and 60 m isobaths at the outer shelf edge of this shoreline makes the FTS one of the most prominent features on the shelf besides the HSV. The HSV/FTS system has significant influence on the cross-shelf transport. The HSV acts both as a conduit for cross-shelf flow as well as a dynamical boundary for along-shelf flow. Winds from the NW can drive a strong up valley return flow along the HSV during the winter mixed season [Harris *et al.*, 2003]. Analysis of CODAR surface current and ADCP mooring data deployed in the HSV during the Langrangian Transport and Transformation Experiment (LaTTE) showed a clear two layer exchange flow during the spring time [Chant *et al.*, 2008]. During the Shallow Water 2006 (SW06) experiment [Tang *et al.*, 2009], satellite Sea Surface Temperature (SST), surface drifters and CODAR surface currents showed that a significant quantity of fresh

riverine water was transported rapidly offshore from the inner shelf to the outer shelf along a pathway south of the HSV [Castelao *et al.*, 2008a]. All of this evidence suggests that the flow in the HSV/FTS region can deviate from the long-term mean shelf-wide flow, depending on the wind and stratification regimes.

### 2.3. Wind Forcing

[6] Wind forcing has long been recognized as an important driver of circulation and transport on continental shelves [Allen and Smith, 1981; Winant, 1980]. Studies of the wind-driven response at the inner shelf have shown that the surface flow is highly correlated with the wind during the stratified season, consistent with an Ekman-type response, and less correlated with the wind when the water column is mixed [Kohut *et al.*, 2004; Dzwonkowski *et al.*, 2009a]. Alongshore winds drive significant cross-shelf transport during the stratified seasons on the North Carolina Shelf [Lentz, 2001] while cross-shore wind is found to be the main driver of surface cross-shelf flow on the inner New England Shelf [Fewings *et al.*, 2008]. Idealized modeling exercises have also shown that cross-shore wind is a significant driver of cross-shelf flow in a weakly stratified water column [Tilburg, 2003]. The different depths and external forcing at the inner and outer shelf result in different dynamical balances reflected in the cross-shelf variability of the shelf flow. Prior studies have focused on the circulation and dynamics at the inner shelf and the outer shelf.

### 2.4. Inner Shelf

[7] The inner shelf dynamics are dominated by buoyancy driven river plumes for most of the year while coastal upwelling becomes more important during the summer time [Song *et al.*, 2001]. Coastal river plumes can carry a high concentration of nutrients and pollutants. The response of a buoyancy trapped river plume, such as the Hudson River Plume, to wind forcing, topography and background flow determines both its initial development [Chant *et al.*, 2008] and downstream evolution [Yankovsky and Garvine, 1998; Yankovsky *et al.*, 2000], which can then affect the whole shelf ecosystem [Schofield *et al.*, 2008]. Extensive research efforts have focused on the effect of upwelling and downwelling favorable alongshore winds on coastal plume dynamics and plume transport [Fong and Geyer, 2001; Chant *et al.*, 2008]. A springtime CODAR virtual drifter study during the Lagrangian Transport and Transformation Experiment (LaTTE) 2005 experiment revealed multiple pathways for Hudson River water leaving the inner shelf Bight apex, either along the Long Island coast, the New Jersey coast, or a cross-shelf pathway south of the HSV [Gong *et al.*, 2006; Zhang *et al.*, 2009]. Coastal upwelling driven by winds from the southwest brings nutrient rich water near the surface, driving summer time primary production at the inner shelf [Glenn *et al.*, 2004]. Alongshore downwelling favorable winds, on the other hand, are associated with development of an alongshore coastal plume [Chant *et al.*, 2008]. Wind-driven Ekman transport associated with coastal upwelling has been proposed as a dominant mechanism for cross-shelf transport from the inner shelf to the outer shelf during the stratified season, with much less influence in the mixed season. [Lentz, 2001].

### 2.5. Outer Shelf

[8] At the outer shelf, the dynamics are dominated by the shelf-slope frontal interactions. The interface between the shelf water and the slope water on the MAB is porous and highly dynamic. A shelf break frontal jet exists at the interface throughout the year, although its structure varies seasonally with changing hydrography [Linder and Gawarkiewicz, 1998]. The equatorward along-shelf transport associated with the shelf break jet is on the order of the shelf-wide transport for the MAB, with stronger summer transport than winter transport observed [Linder and Gawarkiewicz, 1998]. Cross-shelf exchange of shelf and slope water at the shelf break is enhanced during the stratified season when the isopycnals are nearly horizontal from the midshelf to the shelf break. Offshore features such as eddies and Warm Core Rings in the slope sea can modify the velocity structure of the shelf break jet [Gawarkiewicz *et al.*, 2001] and enhance the cross-frontal exchange by pulling surface shelf water offshore and/or bring slope water onshore via subsurface intrusions [Flagg *et al.*, 1994; Hare *et al.*, 2002].

[9] Although there have been case studies of cross-shelf transport pathways on shorter time intervals [Castelao *et al.*, 2008a; Dzwonkowski *et al.*, 2009b], the spatial and temporal variability of the shelf flow is not well known on the seasonal to interannual time scales. The midshelf region and the vicinity of a cross-shelf valley such as the HSV are also much less studied. Furthermore, most previous studies of shelf circulation have divided the shelf into a stratified regime and a mixed regime. That approach misses the flow response to winds and changing stratification during the crucial transition seasons. The transition between the stratified and the well-mixed water column is not instantaneous across the entire shelf, but progresses from shallow to deep water over several weeks or months. A complete seasonal climatology of surface circulation for all four seasons over the full shelf is needed to understand the temporal and spatial variability of shelf-scale transports and their impact on the observed variability in the shelf ecosystem (Y. Xu *et al.*, manuscript in preparation, 2009).

## 3. Methods and Data

### 3.1. Surface Current

[10] The New Jersey Shelf has a cross-shelf distance of 90 to 130 km from the inner shelf to the shelf break and an along-shelf distance of approximately 300 km from the tip of Long Island to Delaware Bay (Figure 1). Surface current data were collected on the New Jersey Shelf from the start of 2002 to the end of 2007 using radial data from three 5 MHz long-range CODAR (Codar Ocean Sensors SeaSonde HF Radar system) sites along the New Jersey coast: Sandy Hook (HOOK), Loveladies (LOVE), and Wildwood (WILD) (Figure 1, black dots). HF Radar uses the Doppler Shift of a radio signal backscattered off the ocean surface to measure the component of the flow in the direction of the antenna [Barrick, 1971a, 1971b; Teague, 1971]. These systems have supported various studies on the New Jersey Shelf including nearshore studies using a 25 MHz standard range system consisting of two shore stations with a coverage area of approximately 30 by 40 km and a resolution of 1.5 km [Kohut *et al.*, 2004, 2006a]. Shelf-wide studies have been

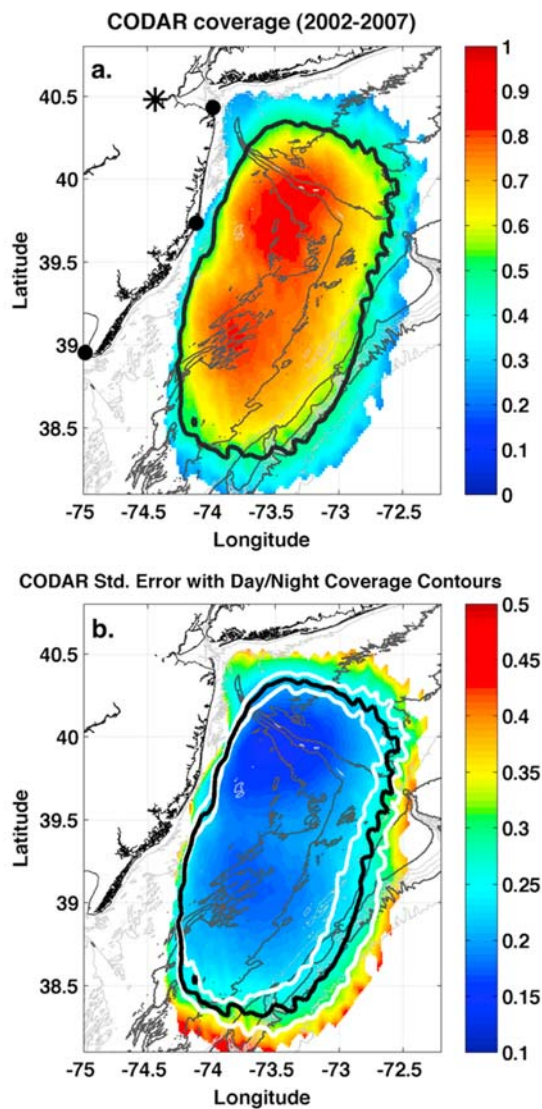


**Figure 2.** (a) Long-range CODAR data coverage for the New Jersey Shelf from 2002 to 2007. The 50% contour is drawn in black. (b) The standard error of the mean current (in cm/s) with day (outer white) and night (inner white) coverage contours.

done using the long-range 5 MHz system consisting of three shore stations with an approximate coverage area of 250 km by 160 km and a resolution of 6 km [Ullman *et al.*, 2006; Hunter *et al.*, 2007; Castelao *et al.*, 2008a; Dzwonkowski *et al.*, 2009a, 2009b].

[11] Hourly radial data from each station are transferred to the Coastal Ocean Observation Lab at Rutgers University, where the radial vector maps (radials) are combined to make 2-D current maps (totals) every 3 hours. Potential ionospheric contamination is eliminated using the manufacturer (CODAR Ocean Sensors) supplied filter applied to each individual Doppler spectra. If ionospheric characteristics are found, data from the entire range cell are removed. Our approach is consistent with the data processing procedures used in previous studies of the New Jersey Shelf [Kohut *et al.*, 2006b; Ullman *et al.*, 2006; Hunter *et al.*, 2007;

Dzwonkowski *et al.*, 2009b]. The resolution of the CODAR radial spectra is dependent on the operating frequency, sweep rate, and FFT length used in processing. Using a standard 1 Hz sweep rate, an operating frequency of 4.55 MHz, and a 1024 point FFT gives a radial velocity resolution of 3.22 cm/s. This operating frequency implies an effective depth of the surface velocity of 2.4 m [Stewart and Joy, 1974]. When radial data from several sites are combined to estimate a total vector, any nonorthogonal angles would introduce some geometric uncertainty. To eliminate less reliable Totals due to poor radial site geometry, we set a threshold for the estimated Geometric Dilution of Precision (GDOP) [Chapman and Graber, 1997]. For this analysis we adopt a community recommended geometric mapping error value of 1.5 or less to identify the vectors with acceptable GDOP [Dzwonkowski *et al.*, 2009a]. This value is chosen based on current comparison studies using CODAR and ADCPs [Kohut *et al.*, 2006a] and CODAR and drifters [Ohlmann *et al.*, 2007]. These studies show that when subgrid-scale spatial variability is accounted for, the adjustable CODAR current resolution is matched to the uncertainty level in the observed currents. The spatial resolution of the final total vector current maps is 6 km with a cross-shelf range of 150 km. The averaged current fields are constructed using the 3 hourly total vector maps. A minimum of 50% temporal coverage over the entire 6 year record is required to be included in the following analysis (Figure 2a).

[12] Diurnal differences in the CODAR coverage area do occur due to the increase in the background noise levels at night. To assess their potential impact, the standard error of the mean flow was calculated for the full field. The 50% coverage line for the larger day time and smaller nighttime fields are added to the standard error plot in Figure 2b. In all cases, the standard error remains in the range of 0.25 to 0.35 cm/s with little difference from the intermediate value chosen for this study. The HF Radar coverage area is also affected by the roughness of the sea state, which has been shown to increase with larger wind waves [Barrick, 1971a]. The theoretical study of Barrick [1971a] showed that the returned signal is enhanced in stronger winds up to 15 knots for HF Radar systems operating below 10 MHz. On average, persistent NW winds during winter are stronger than SW winds during summer [Moore *et al.*, 1976]. As a result the CODAR coverage area is often increased during the windy winter compared to the calmer summer.

[13] All CODAR surface currents are detided using the T\_TIDE Matlab package [Pawlowicz *et al.*, 2002] before further analysis is performed. Since the outer shelf is least affected by the diurnal variations of sea/land breeze due to its distance from shore [Hunter *et al.*, 2007], and the time scale of our study is from monthly to interannual averaging over many tidal, diurnal and inertial cycles, we believe that the higher-frequency effects of diurnal coverage difference, sea/land breeze, and tidal/inertial influences will not measurably bias the result of our present study.

### 3.2. Winds

[14] Wind data from five NOAA NDBC buoys (ASLN6, 44025, 44009, 44017, 44004) including four on the New Jersey Shelf and one offshore in the slope sea (44004) are used for the wind analysis (Figure 1, open diamonds). Cross correlations of the 5 buoys are performed on low-pass filtered (Hamming filter with a 33 hour window) hourly wind

**Table 1.** NDBC Buoy Wind Cross-Correlation Magnitudes

Wind Cross Correlation	ASLN6	44025	44009	44017	44004
ASLN6	1.00	0.82	0.72	0.84	0.56
44025		1.00	0.80	0.82	0.64
44009			1.00	0.79	0.70
44017				1.00	0.51
44004					1.00

data over the 6 years from 2002 to 2007. The cross-correlation coefficients and the temporal lags of the wind velocity among the five buoys are tabulated in Tables 1 and 2, respectively. Over the length scale of the New Jersey Shelf, winds are highly correlated ( $>0.7$ ) at subtidal time scales among all four sites on the shelf (Table 1). The southern buoys lead the northern buoys and the inshore buoys lead the offshore buoys in time on the order a few hours (Table 2). The observed temporal lag is consistent with the fact that most frontal systems propagate northeastward on the MAB shelf. The velocity correlation of shelf wind buoys with the offshore wind buoy are weaker, but are still greater than 0.5 between all sites. The correlation analysis suggests that under many conditions, the wind field of the Mid-Atlantic Bight region had a correlation scale at least the size of the New Jersey Shelf. For the analysis presented in sections 4.1–4.7, we will be focusing on wind data from NOAA NDBC Buoy 44009 (38.46 N 74.70 W) due to its good temporal coverage and proximity to the center of the study region near the Tuckerton Endurance Line.

## 4. Results

### 4.1. Mean Current and Variability

#### 4.1.1. Mean

[15] The mean surface flow on the New Jersey Shelf over a period of 6 years (2002–2007), as measured by the Rutgers long-range CODAR network, is generally offshore and down shelf with a speed of 3–12 cm/s (Figure 3a). The mean surface flow contained along-shelf and cross-shelf flow structures with velocity ranges from 2 cm/s at the inner shelf, to 6 cm/s at the midshelf, to 12 cm/s at the shelf break. The weakest flow regions, with a speed of 3 cm/s or less, are observed at the inner to midshelf south of the Hudson Shelf Valley (HSV) and in an area north of the HSV. A band of higher-velocity flow 30 to 50 km wide, with an average current speed of 5–7 cm/s, is seen just to the south of the HSV. The fastest surface flow is seen offshore of the 80 meter isobath near the shelf break (8–12 cm/s). Just north of the HSV, the flow is weakly down shelf toward the SW. South of the HSV at the inner shelf, the flow is offshore, directed toward the SE. At the outer shelf, the flow veered clockwise heading down shelf toward the SW. The mean surface flow is largely consistent with the along-isobath, equatorward depth-averaged flow as measured by current meter moorings [Beardsley and Boicourt, 1981; Lentz, 2008a].

[16] The HSV appears to separate the flow regimes geographically and exert topographic control over local circulation. There is a clear difference in the surface current velocities between regions to the north and to the south of the HSV, with enhanced flow velocity observed to the south compared to the north (Figure 3a). A divergence map of the

mean surface flow illustrates that the 6 year mean flow is divergent over the HSV and north near the midshelf and convergent south of the HSV (Figure 3b). The persistent divergence zone suggests an enhanced upwelling of subsurface material. In regions away from the influence of the HSV, the along-shelf component of the flow velocity increases linearly with the water column depth, a result consistent with a simple 2-D shelf model assuming geostrophic balance plus wind forcing for the along-shelf direction [Csanady, 1976; Lentz, 2008a]. The flow in these regions shows no coherent structure in the divergence, though the amplitude of the divergence fluctuations is of the same order of magnitude as the HSV region.

#### 4.1.2. Variability

[17] Consistent with historical current meter analysis [Beardsley and Boicourt, 1981], the variability in the surface current is significant compared to the mean. The root mean square (RMS) of the detided surface current ranges from 11 cm/s at the upper portion of the HSV to 17 cm/s at midshelf regions to the south of the HSV (Figure 3c). Two regions of high variability are noted, one centered along the 40 m isobath near 39.5 N, 73.5 W just south of the HSV, and the other located further to the south near latitude 38.5 N, with RMS of 17 to 20 cm/s. Near the HSV, on the other hand, the RMS speed has much lower values of 12 to 15 cm/s. The average RMS for the whole field is 15.5 cm/s.

[18] Different forcing mechanisms can affect the spatial variability at different scales. Earlier analyses of the spatial correlation of winds and different seasonal stratification suggest that coherent wind forcing and stratification operate at shelf-wide scales while the shelf topography can vary on scales of a few kilometer to tens of kilometers, a fraction of the shelf size. For temporal variability, we hypothesize that wind forcing is the dominant factor after the tidal contribution has been removed. The RMS current speed for the low-wind conditions from 2002 to 2007 with an average value of 12.2 cm/s (Figure 3d) is significantly lower than the total RMS (Figure 3c). In sections 4.3–4.5 we examine how different wind conditions and changing stratification affect the temporal and spatial variability of the surface circulation in the New Jersey Shelf. The first step is to determine the topographically modulated background flow in the absence of winds so that the effect of large-scale forcing can be separated from that of the winds and stratification.

### 4.2. Background Flow and Topography

[19] The large-scale along-shelf flow over the length of the MAB has long been observed [Bumpus, 1973; Beardsley et al., 1976]. Since the very early studies of the MAB shelf, the along-shelf flow has been hypothesized to be driven by a large-scale along-shelf pressure gradient imposed at the shelf break [Csanady, 1976] setup by the large-scale circulation in

**Table 2.** NDBC Buoy Wind Cross-Correlation Time Lags<sup>a</sup>

Wind t Lag (days)	ASLN6	44025	44009	44017	44004
ASLN6	0	-1	1	-3	-5
44025		0	2	-2	-4
44009			0	-4	-6
44017				0	-2
44004					0

<sup>a</sup>Time lag is given in hours.

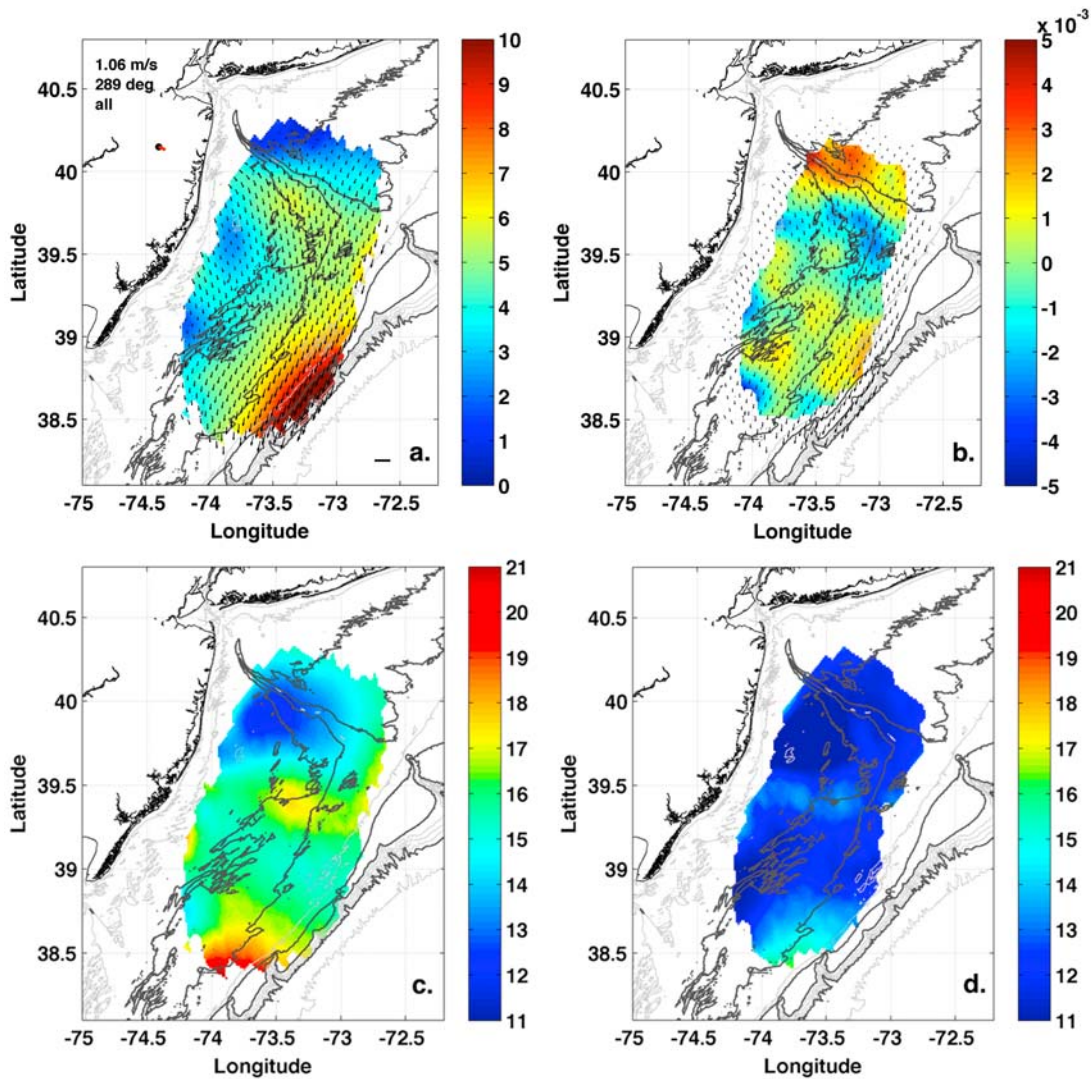


**Figure 3.** (a) Mean surface current for New Jersey Shelf (2002–2007) in cm/s. Average wind speed (m/s) and direction (degrees from true north) measured by NOAA NDBC Buoy 44009 is given. (b) Divergence map of the CODAR mean surface current (2002–2007) in 1/hour. (c) RMS of the detided surface current from 2002–2007. Color bar indicates current speed in cm/s. (d) RMS current speed for weak wind conditions when winds were less than 2 m/s.

the western North Atlantic [Beardsley and Winant, 1979]. Such a background flow would exist on the shelf in the absence of wind and other local forcing such as river discharge. To calculate an estimate of the background shelf surface flow due to the large-scale along-shelf pressure gradient, the 2002–2007 surface current data was averaged conditionally for winds less than 2 m/s (Figure 4a). The directional distribution of the winds in this weak wind regime is approximately uniform for all seasons with a mean wind speed of 0.1 m/s. The effect of the sloping cross-shelf topography is clearly seen in the background surface flow, away from the HSV/FTS. The along-shelf flow speed increases from 2–4 cm/s at the inner shelf to 6–10 cm/s at the outer shelf. Compared to the 6 year mean field (Figure 3a), the low-wind flow field has a weaker offshore flow component at the inner to midshelf.

[20] Assuming maximum velocities of 6–10 cm/s (Figure 4a),  $f = 10^{-4} \text{ s}^{-1}$  and a curvature length scale of  $L \sim 50 \text{ km}$  derived from the maximum curvature of the flow along the axis of the HSV, the Rossby number of the flow is  $Ro = U/fL = 0.025$  or less. This indicates a geostrophic balance dominating these low-wind regimes. Even for the larger flow speeds of 30 cm/s occasionally observed on the shelf under strong wind conditions, the Rossby number remains small and less than 0.1, indicating that the nonlinear advective terms in the momentum equation do not contribute significantly to the momentum balance over the seasonal time scale.

[21] A two-dimensional model for the mean circulation on the MAB that assumed a geostrophic balance in the cross-shelf direction and an Ekman balance in the along-shelf direction produced a depth-averaged along-shelf velocity

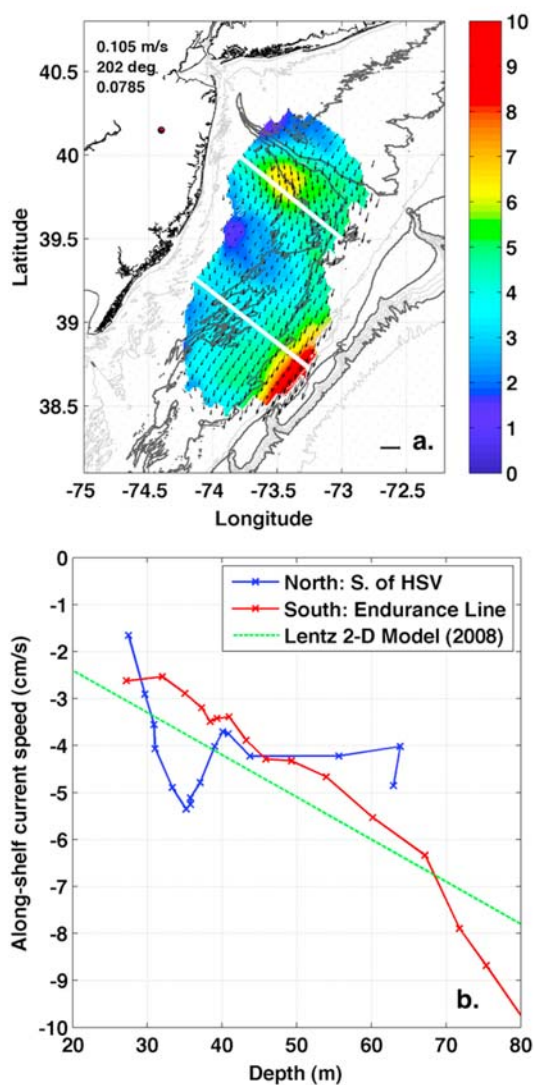


**Figure 4.** (a) Mean surface current field for weak wind conditions ( $<2$  m/s) for 2002–2007 in cm/s. The mean wind speed, direction, and fraction of the total time are listed. (b) Comparison of along-shelf velocity for a cross-shelf section just south of HSV (blue) and another south of the Tuckerton Endurance Line (red). The depth-averaged along-shelf flow velocity given by a 2-D shelf model is shown in green.

that is a linear function of the depths of the isobaths [Csanady, 1976; Lentz, 2008a]. To evaluate the dynamical importance of winds below 2 m/s, we compare the contributions to the momentum equation by the large scale pressure gradient ( $g\theta$ ) and by the mean wind stress ( $\tau/\rho_0h$ ) for winds below 2 m/s, where  $\theta = \Delta\eta/\Delta y$  is the slope of sea surface,  $\tau$  is the wind stress and  $h$  is the depth of the surface mixed layer. Using a mean along-shelf sea surface slope of  $3.7 \times 10^{-8}$  as estimated by Lentz [2008a], a mean wind stress of  $1.5 \times 10^{-5}$  N/m<sup>2</sup> (corresponding to a mean wind speed of 0.1 m/s) and a surface mixing layer thickness of  $h = 15$  m, the pressure gradient contribution to the momentum equation of  $3.6 \times 10^{-7}$  m/s<sup>2</sup> is over 2 orders of magnitude larger than the wind stress contribution of  $10^{-9}$  m/s<sup>2</sup>, suggesting that the uniformly distrib-

uted winds below 2 m/s do not significantly affect the shelf momentum balance.

[22] Topographic features such as the HSV and FTS can modify the shelf flow by introducing along-shelf variability. In the low-wind background current field, the flow velocity is enhanced at the midshelf just to the south of the HSV and FTS (Figure 4a). The surface along-shelf velocity for two cross-shelf transects is calculated from the low-wind background mean field described above. One transect is just south of the HSV and the other transect is further south near the Tuckerton Endurance Line. The cross-shelf velocity profiles as a function of depth for the two transects are compared with the 2-D model result of Lentz [2008a] (Figure 4b). The linear 2-D model (green line) has a slope of  $-0.09$  cm s<sup>-1</sup> m<sup>-1</sup> and an intercept of  $-0.6$  cm/s, within the range of parameter uncertainty provided by Lentz [2008a]. The different flow dependence on water depth is noted for the two transects with different cross-shelf topography. The along-shelf flow across the northern HSV transect (blue), is significantly different from the linear 2-D model (green). The observed flow exhibits a nonmonotonic dependence on the depth of the isobath with a maximum in along-shelf velocity observed at the midshelf just to the south of the HSV. The southern transect, on the other hand, has an along-shelf current speed that is nearly a linear function of depth out to the 70 m isobath (red). Offshore of the 70 m isobath, the linear relationship still holds but the flow speed's dependence on depth has a steeper slope. This increase in along-shelf speed seaward of the 70 m isobath is likely due to the effect of the shelf slope frontal jet meandering onto the outer shelf near the edge of the CODAR coverage. The shelf-slope frontal jet is not included in the model of Lentz [2008a].

[23] The direction and the general features associated with this background flow do not change with the seasons, although the magnitude of the flow in the seasonal low-wind field can vary up to 3 cm/s compared to the multiyear mean. Specifically there is enhanced down-shelf flow at the outer shelf in the autumn and just south of the HSV in the winter. For the majority of the shelf and for most of the year, the variability in the low-wind background flow is less than 2 cm/s. The weak winds condition is not common on the shelf, occurring on average 8% of the time. Over the seasonal time scale, the weak wind condition is more frequent in the summer occurring 10% of the time and significantly less frequent in the winter occurring only 4% of the time. Over the interannual time scale, the annual average of the low-wind condition ranges between 6% of the time and 12% of the time over a 20 year period from 1987 to 2007.

[24] Before investigating the surface flow response to winds and stratification on the New Jersey Shelf, we want to remove the effect of the topographically modulated pressure gradient driven background flow using the calculated low-wind mean surface current as a representation of the surface response to the large-scale along-shelf forcing. The multi-year averaged low-wind mean is used as the background field because the observed seasonal variability of the low-wind current is relatively small and the enhanced coverage gained by combining the limited amount of low-wind data is significant. The calculated background field is then subtracted from the surface current data in our Eulerian analysis

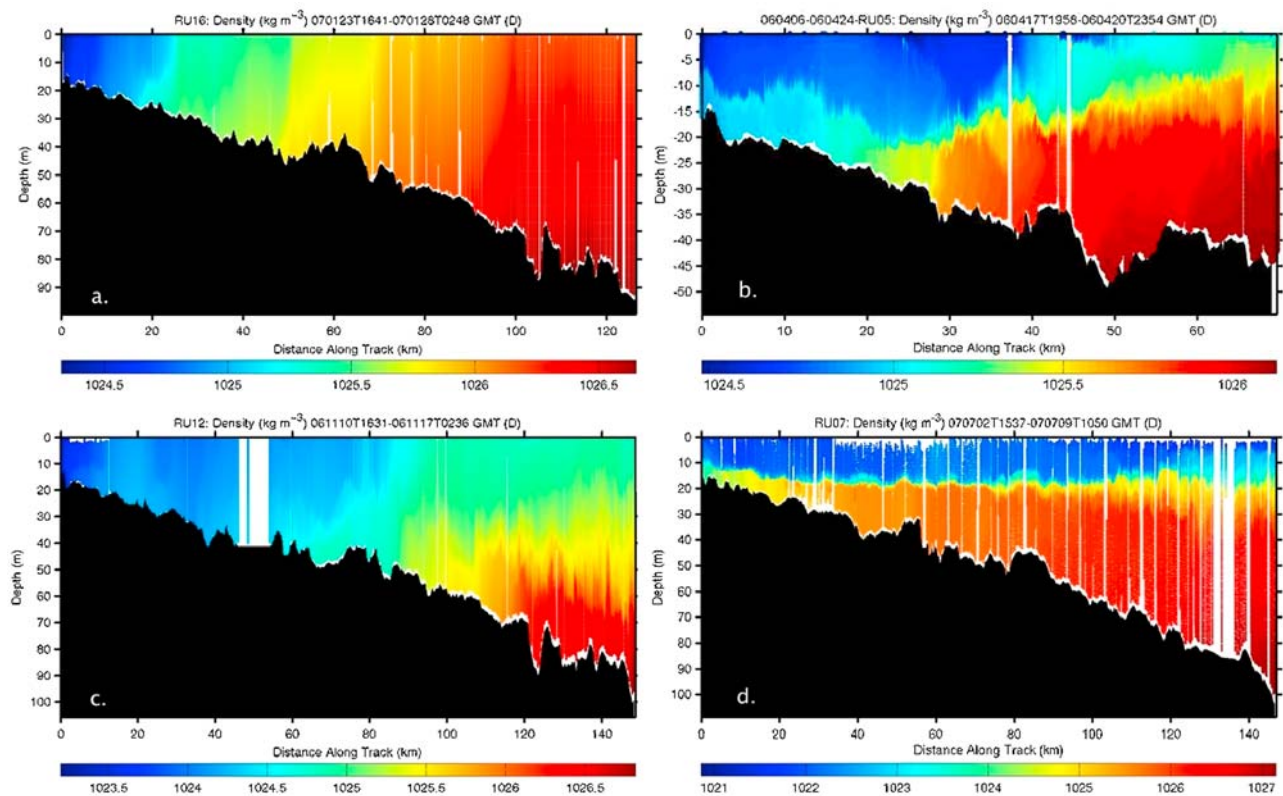


**Figure 5.** New Jersey Shelf seasonal density sections along the Tuckerton Endurance Line ( $\text{kg}/\text{m}^3$ ): (a) unstratified winter (December–February), (b) stratifying spring (March–May), (c) destratifying autumn (September–November), and (d) stratified summer (June–August).

of seasonal wind-driven circulation (section 4.4 and 4.5). This approach enables us to look more directly at the spatial and temporal structure of the flow response associated with the surface wind forcing from various directions and under different stratification regimes.

#### 4.3. Stratification, Wind, and Seasonal Flow

[25] While many factors contribute to the variability of the surface currents, two significant forcing factors are stratification and wind [Beardsley and Boicourt, 1981; Kohut et al., 2004; Lentz, 2001; Dzwonkowski et al., 2009b]. The New Jersey Shelf undergoes an annual cycle ranging from intense stratification in the summer to mixed conditions in the winter [Bigelow, 1933; Bigelow and Sears, 1935; Castelao et al., 2008b; Schofield et al., 2008]. The changes in the water column's density structure can affect the vertical transfer of momentum, which in turn can affect the current's response to wind forcing. Wind stress is highly variable on the shelf in the synoptic band (2–10 days) due to broadband atmospheric transients [Beardsley and Boicourt, 1981]. Seasonal variability of stratification and wind forcing can have significant effect on the seasonal flow, which is characterized by calculating the mean surface current for each of the seasons for the six years from 2002 to 2007.

[26] Representative hydrographic sections from the Tuckerton Endurance Line [Castelao et al., 2008b] for each of the four seasons are shown in Figure 5. The summer months are highly stratified, characterized by a strong thermocline at middepth. In the cooler, windy winters the water

column is well mixed. For the transition seasons, the water column is stratifying in the spring from seasonal heating and increased river runoff and destratifying in autumn due to seasonal cooling and storm-induced mixing. The four seasons are defined as by Flagg et al.'s [2006] climatological analysis of the outer shelf currents, a reasonable choice based on our historic knowledge of the MAB [e.g., Bigelow, 1933], recent analysis of the seasonal variability in the New Jersey Shelf hydrography [Castelao et al., 2008b], and our own climatological analysis of winds from NOAA NDBC Buoy 44009 (1987–2007, outside Delaware Bay; Figures 6 and 7).

[27] Winter, from December to February, is characterized by a well-mixed water column [Castelao et al., 2008b] and the prevalence of NW winds blowing across the shelf [Mooers et al., 1976]. A sample glider cross-shelf density transect during the month of January shows the typical winter time New Jersey Shelf density structure (Figure 5a). The 2-D histogram of wind speed and wind direction for 2002–2007 indicates that the frequency of NW winds was highest during the winter season, occurring on average 41% of the time (Figure 6a). Over the period from 1987 to 2007, the relative frequency of NW winds varies from 30% in 1998 to 53% in 2007 (Figure 7a). For all years except 1990 when SW winds were dominant, NW is the dominant wind direction for the winter mixed season. The wintertime mean surface flow has three notable characteristics (Figure 8a). First, in the region south of the HSV, the southward flow is nearly spatially uniform and directed offshore and down shelf. The flow velocity is  $\sim 6$  cm/s for most of the shelf except at the outer

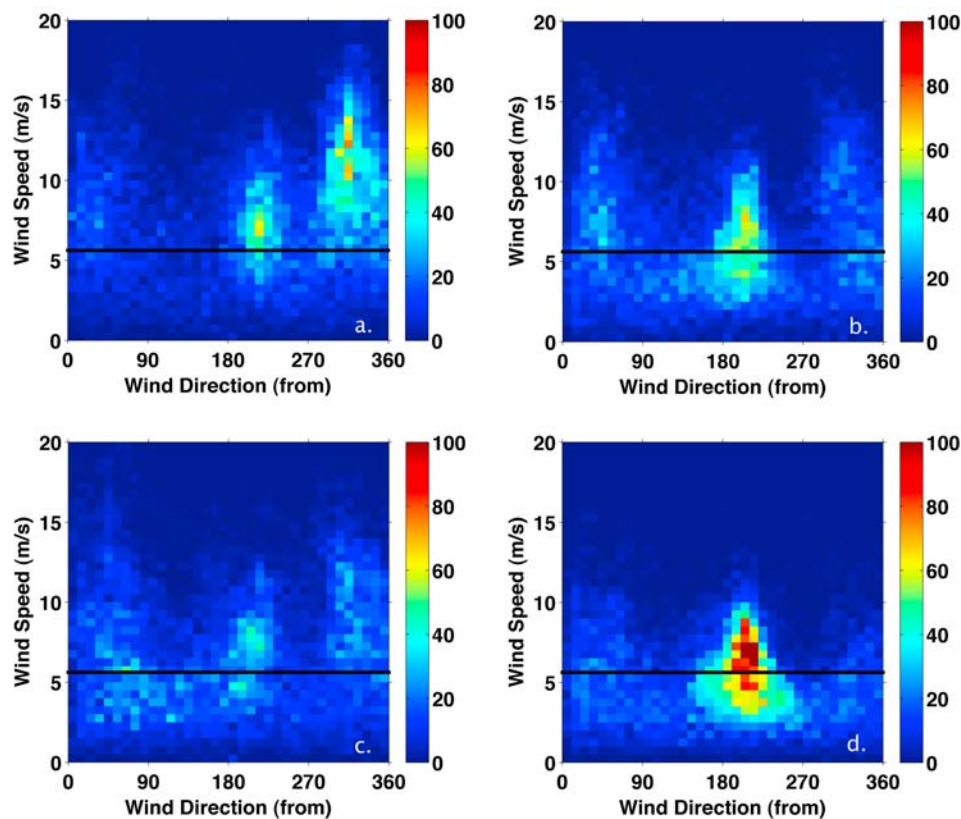


**Figure 6.** Histogram of hourly winds by season with color bar indicating number of occurrences. The black lines represent a wind stress of  $0.05 \text{ N/m}^2$ : (a) winter (December–February), (b) spring (March–May), (c) autumn (September–November), and (d) summer (June–August).

shelf region. Second, along the outer shelf seaward of the 80 m isobath at the shelf break, the surface flow speed increases to greater than  $13 \text{ cm/s}$  while the flow direction turns along shelf. Third, in the region north of the HSV, the current velocity is very weak ( $<3 \text{ cm/s}$ ). Over most of the shelf, the surface flow over seasonal scales is wind-driven except for the area near the HSV and the shelf break where topographic steering effects become important and baroclinic forcing drives a shelf-slope frontal jet. Compared to the long-term mean (Figure 3a), the wintertime flow has a significantly higher cross-shelf flow for most of the shelf except for the region near the HSV and just to the south where it was similar to the mean.

[28] Spring, from March to May, is characterized by the transition from a well-mixed water column to a more stratified water column. During most years the highest freshwater river discharge onto the shelf also occurs during the spring season [Chant *et al.*, 2008]. A sample glider cross-shelf transect from April shows a partially stratified water column with significantly more of the lower-density riverine water appearing on the shelf (Figure 5b). During spring, the wind pattern is less stable than either the stratified or the mixed season. The weakening NW winds give way to more frequent but lower-energy along-shore NE and SW winds (Figure 6b), occurring on average 21 and 32% of the time, respectively. The spring wind pattern can vary significantly on the inter-annual time scale. NW winds can occur 8% (1991) to 28% (1997) of the time, NE winds can occur 10% (1997) to 38% (1987) of the time, while SW winds can occur 17% (1992)

to 44% (1991) of the time (Figure 7b). The causes of such interannual variability are likely associated with variability in the large-scale atmospheric circulation pattern and the frequency of storms. NE winds tend to drive along-shelf, down-shelf flow. The 6 year climatology of seasonal flow on the shelf during the spring is directed mostly down shelf toward the southwest with a speed of 3 to 7  $\text{cm/s}$  (Figure 8b). A large portion of the area to the south of the HSV has a velocity of less than  $5 \text{ cm/s}$ . Near the shelf break, offshore of the 100 m isobath, the current velocity increases significantly to over  $15 \text{ cm/s}$ . The increased alongshore wind forcing combined with buoyancy forcing due to increased river discharge results in favorable conditions for along-shelf transport during the spring. Compared to the long-term mean, springtime flow has weaker offshore flow, especially in the region south of the HSV and inshore of the 40 m isobath.

[29] Summer, from June to August, is characterized by a highly stratified water column. As shown in the sample cross-shelf density section (Figure 5d), the stratified surface layer is 10 to 25 meters thick. The density difference between the surface and bottom layers could be as large as  $6 \text{ kg/m}^3$ , sometimes higher. The overall wind strength for the summer season is weaker than all the other seasons. The wind direction is predominately along-shore from the upwelling favorable SW, occurring 48% of the time (Figure 6d). This SW wind pattern varies little interannually ranging from 30% in 1998 to 55% in 1988 (Figure 7d). NE winds are the second most common direction during the summer, with occurrences ranging from 7% (1994) to 22% (1995) of the time, and

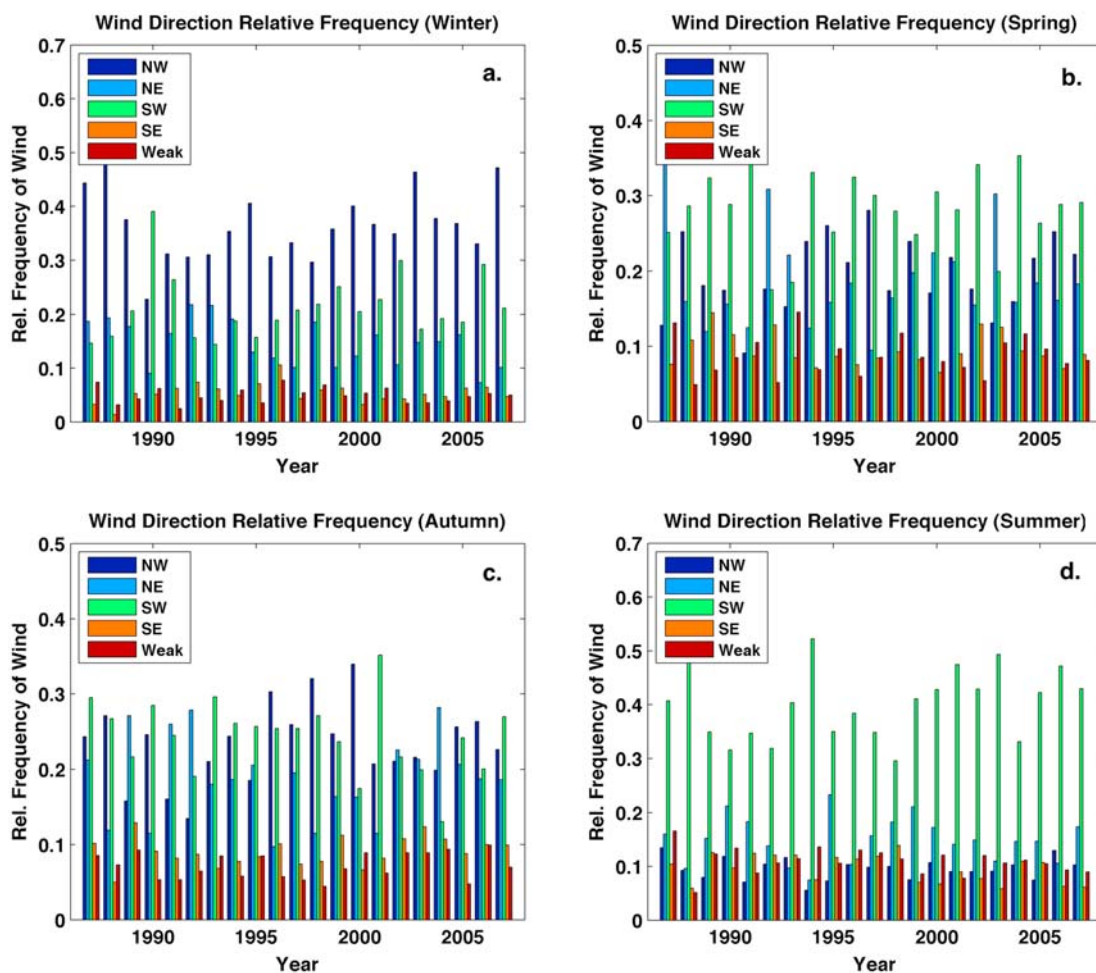


**Figure 7.** Interannual variability of the relative frequency of NW, NE, SW, SE, and weak (less than 2 m/s) winds for NOAA NDBC Buoy 44009: (a) winter (December–February), (b) spring (March–May), (c) autumn (September–November), and (d) summer (June–August).

averaging 15% of the time between 2002 and 2007. The climatology of mean surface currents for the summer season from 2002 to 2007 includes a continuous band of stronger flow on the shelf (Figure 8d), starting with the region just south of the Hudson Shelf Valley stretching from the inner shelf to the outer shelf with the flow directed mostly cross shelf. This cross-shelf flow connects with faster offshore flows seaward of the 60 m isobath, where the flow is directed more along-shelf with a velocity of 7–9 cm/s. The surrounding regions, in particular the region north of the HSV and the region in between the 40 and 60 m isobath to the south, has down-shelf surface current speeds weaker than 5 cm/s, directed down shelf to the SW. Shoreward of the 40 m isobath, the current velocity drops to nearly zero. The increased offshore flow is qualitatively consistent with a SW wind driving a coastal upwelling system on the shelf. The summertime flow structure over the HSV and offshore is similar to that of the long-term mean, but the flow at the inner shelf has a weaker along-shelf component compared to the overall mean.

[30] Autumn, from September to November, is characterized by frequent storms that break down the summer stratification. The cooling of the surface layer preconditions

the water column for storm mixing. A warm and salty surface layer tends to overlay a cold and fresher bottom layer during autumn on the New Jersey Shelf. Eventually increased storm activity mixes away the remaining stratification. A sample density cross-shelf section from November shows that the stratification of the water column had already broken down at the inner shelf and is reduced at the mid- to outer shelf (Figure 6c). During this time, the winds shift from the weaker SW winds of the summer (23% of the time between 2002 and 2007) to the stronger and more frequent NE and NW winds associated with passing fronts and storms occurring 24% and 25% of the time (between 2002 and 2007), respectively (Figure 6c). There is significant variability in their relative frequency over the interannual time scale. Over the twenty year period from 1987 to 2007, the occurrence of autumn SW winds ranged from 13% (2004) to 35% (2001), the occurrence of NW winds ranged from 13% (1992) to 34% (2000), and the occurrence of NE winds ranged from 10% (1996) to 28% (1992 and 2004) (Figure 7c). The frequent NE winds drive energetic along-shelf and onshore flow. The seasonal mean surface current map shows three distinct flow regions (Figure 8c). North of the HSV, there is weak flow with

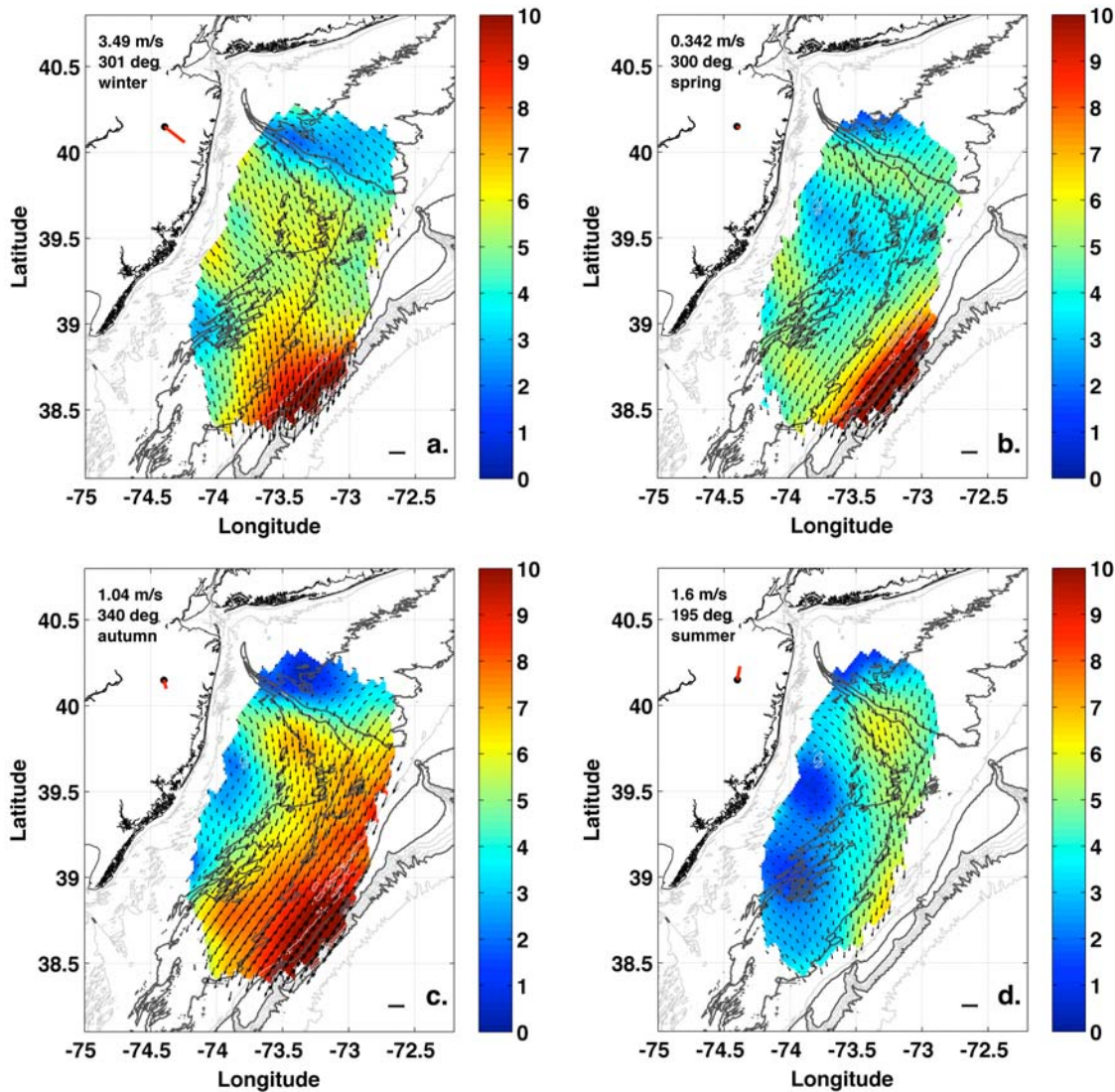


**Figure 8.** Seasonal surface current on the New Jersey Shelf (cm/s): (a) winter (December–February), (b) spring (March–May), (c) autumn (September–November), and (d) summer (June–August).

speeds less than 3 cm/s. The mid to outer portion of the shelf south of the HSV includes a broad band of strong along-shore, down-shelf flow with the highest seasonal mean velocity of any of the seasons, averaging 8–10 cm/s. The current at the inner shelf region south of the HSV is weak with velocities less than 5 cm/s. Compared to the long-term mean, the autumn down-shelf flow is significantly higher at the mid and outer shelf in the region south of the HSV.

#### 4.4. Wind-Driven Circulation

[31] We next calculate the mean spatial response of the surface circulation on the New Jersey Shelf to wind forcing and seasonal changes. The low-wind mean is used as an estimate of the nonwind driven background component of the surface circulation, which is then subtracted from the conditionally averaged fields to obtain the wind-only component of the surface flow for different wind regimes. The response of the ocean surface to each wind regime for the different seasons with the background low-wind mean

removed are shown in Figures 9–12. At a first glance, the surface flow is largely in the direction of the wind during the winter when the water column is well mixed and more to the right of the wind during the summer when the water column is highly stratified. For the transition seasons of spring and autumn, the wind driven response of surface flow is in between the angular range of the winter and summer scenarios. To characterize the effect of wind forcing on the current variability for all the seasons, the spatially averaged RMS/Mean for each case of the wind-based conditionally averaged flow are computed and presented in Table 3. The total RMS/Mean for all seasons and all wind directions is 3.3. In general the variability of the current compared to the mean is much lower for wind-driven flows with RMS/Mean ranging from 1.1 under NE winds to 1.8 under SW with the exception of SE winds (with a value of 3.5) because the average flow is very weak under those conditions. In some cases such as under NE winds during winter and spring, the RMS/Mean is less than 1. This result confirms that wind

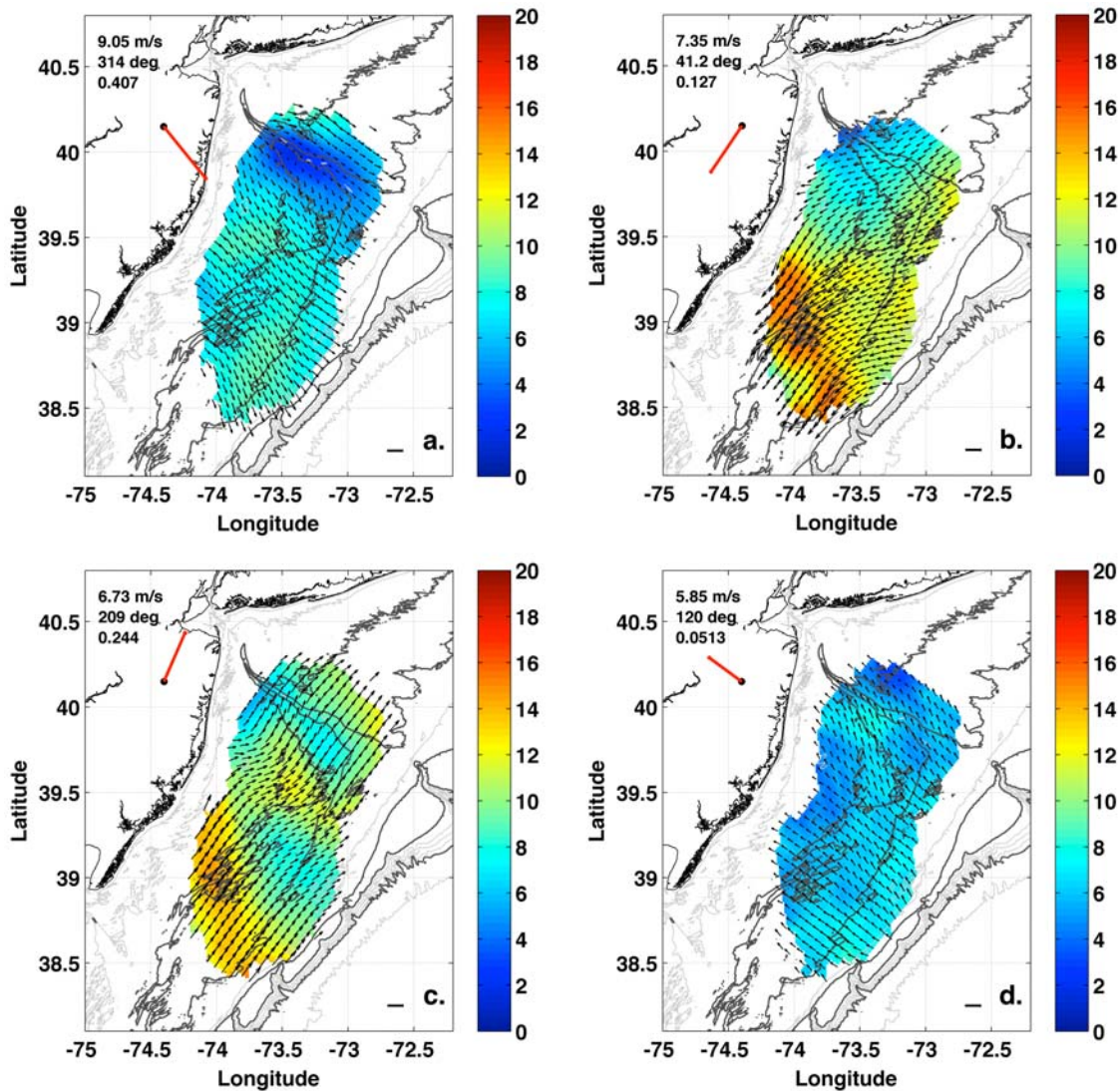


**Figure 9.** Winter mean current based on wind (cm/s): (a) northwest winds, (b) northeast winds, (c) southwest winds, and (d) southeast winds.

forcing variability is the dominant source of subtidal temporal variability for the shelf surface flow.

[32] The surface flow responses to winter wind forcing are shown in Figure 9. Winter is characterized by strong NW winds, which occur 41% of the time with a mean velocity of 9.1 m/s ( $0.13 \text{ N/m}^2$ ), followed by SW winds which occur 24% of the time with a mean velocity of 6.73 m/s ( $0.072 \text{ N/m}^2$ ). Under the cross-shore NW winds, the surface flow is cross shelf in the offshore direction (Figure 9a). However, despite the strong wind forcing, the flow velocity over the HSV and the nearby region remain weak with mean current speeds of less than 5 cm/s. Nevertheless, winter can be a season of significant cross-shelf transport due to frequent NW winds driving cross-shelf flow. Southward of the offshore tip of the FTS, the flow velocity increases to 8 cm/s. The shelf-wide offshore flow south of the HSV has little cross-shelf variability, suggesting a depth-independent wind-driven response of the unstratified water column. Under wintertime SW winds, the surface flow is essentially up shelf toward the NE with a speed of 8–14 cm/s (Figure 9c). An offshore veering is

observed as the flow reaches the southern side of the FTS. For the two less common wind regimes, NE winds (13% of the time) drive along-shore, down-shelf flow with speeds of 7–16 cm/s (Figure 9b), and SE winds (5% of the time) drive onshore, up-shelf flow with speeds of 3–7 cm/s for most of the shelf (Figure 9d).

[33] The surface flow responses to different spring wind forcing regimes are shown in Figure 10. Spring is characterized by the weakening of NW winds and a corresponding increase in the frequency of NE and SW winds. NW winds, common in the early part of spring, occur 21 percent of the time with a mean wind speed of 7.2 m/s. Under such wind forcing, the surface flow is largely cross shelf for the southern portion of the New Jersey Shelf. The flow is similar to what was observed during the winter but with an expanded low-speed zone that includes the whole HSV and FTS area. The combination of the weakening of the cross-shelf NW wind and shrinking area of the cross-shelf flow suggest less offshore transport during the spring. SW winds, more common in late spring, occur 32% of the time with a mean speed of

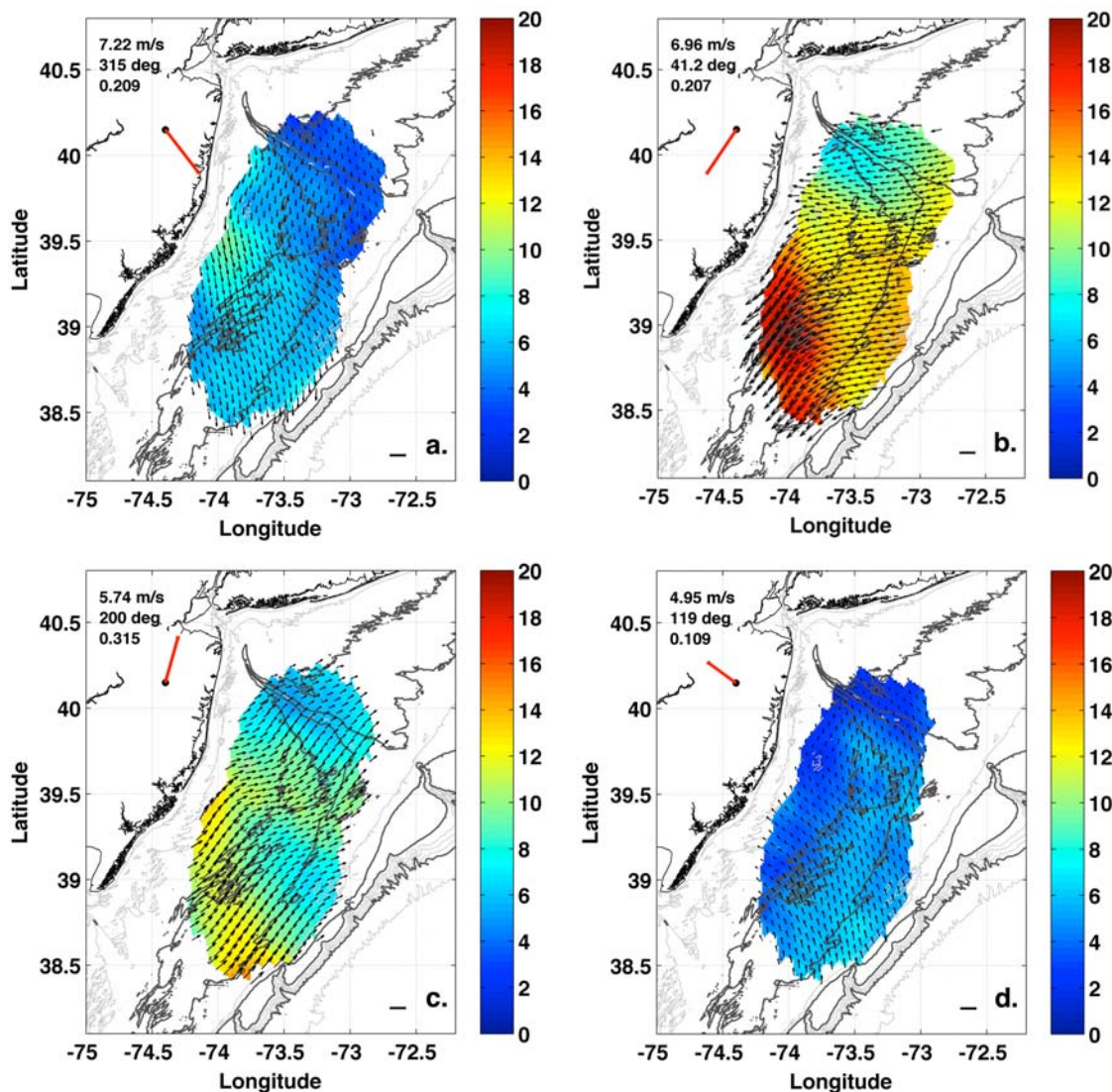


**Figure 10.** Spring mean current based on wind (cm/s): (a) northwest winds, (b) northeast winds, (c) southwest winds, and (d) southeast winds.

5.7 m/s (Figure 10c). It generates an along-shore up-shelf flow pattern that is largely similar to that of the wintertime case. The alongshore NE winds, which occur 21% of the time with a mean velocity of 6.96 m/s, generate the most energetic flow response of the spring. The surface current speeds range from 8 cm/s near the HSV to over 20 cm/s near the Tuckerton Endurance Line (Figure 10b). Just south of the HSV, over the FTS region, the flow is mostly onshore. Further south near the Tuckerton Endurance Line, the flow turns alongshore at the inner shelf (Figure 10b). The counterclockwise veering of the flow under NE winds is observed for much of the southern region approaching the inner shelf from offshore.

[34] The surface flow responses to different summer wind forcing regimes are shown in Figure 11. The summer stratified season is the least energetic of all the seasons. Nearly 48% of all winds are along-shore SW winds with a mean speed of 5.3 m/s. SW winds tend to drive up-shelf flow at the inner shelf and cross-shelf offshore flow at the mid to outer shelf (Figure 11c). The flow over the HSV is

the weakest with a speed of 7 cm/s, while the flow at the inner shelf and over the FTS south of the HSV is the strongest with a speed of 10–12 cm/s. Of the three other wind regimes during the summer, NE winds, occurring 15% of the time with a mean speed of 5.5 m/s, drive a nearly on-shore flow with a slight down-shelf component (Figure 11b). NW winds, occurring 11% of the time with a mean speed of 4.57 m/s, drive a down-shelf flow of 5 to 10 cm/s. SE winds, occurring 9% of the time with a mean speed of 4.4 m/s, interestingly stop nearly all wind-driven components of the surface flow on the shelf (Figure 11d).

[35] The surface flow response to autumn wind forcing regimes are shown in Figure 12. Surface flow during autumn is the most energetic of all the seasons. With the arrival of autumn, decreasing surface temperature and increased storm frequency enhance the vertical mixing of the water column. The wind regime undergoes a transitional phase from weak SW winds to strong NE winds often generated by storms. Winds from all three principal directions, NW, SW, and NE,

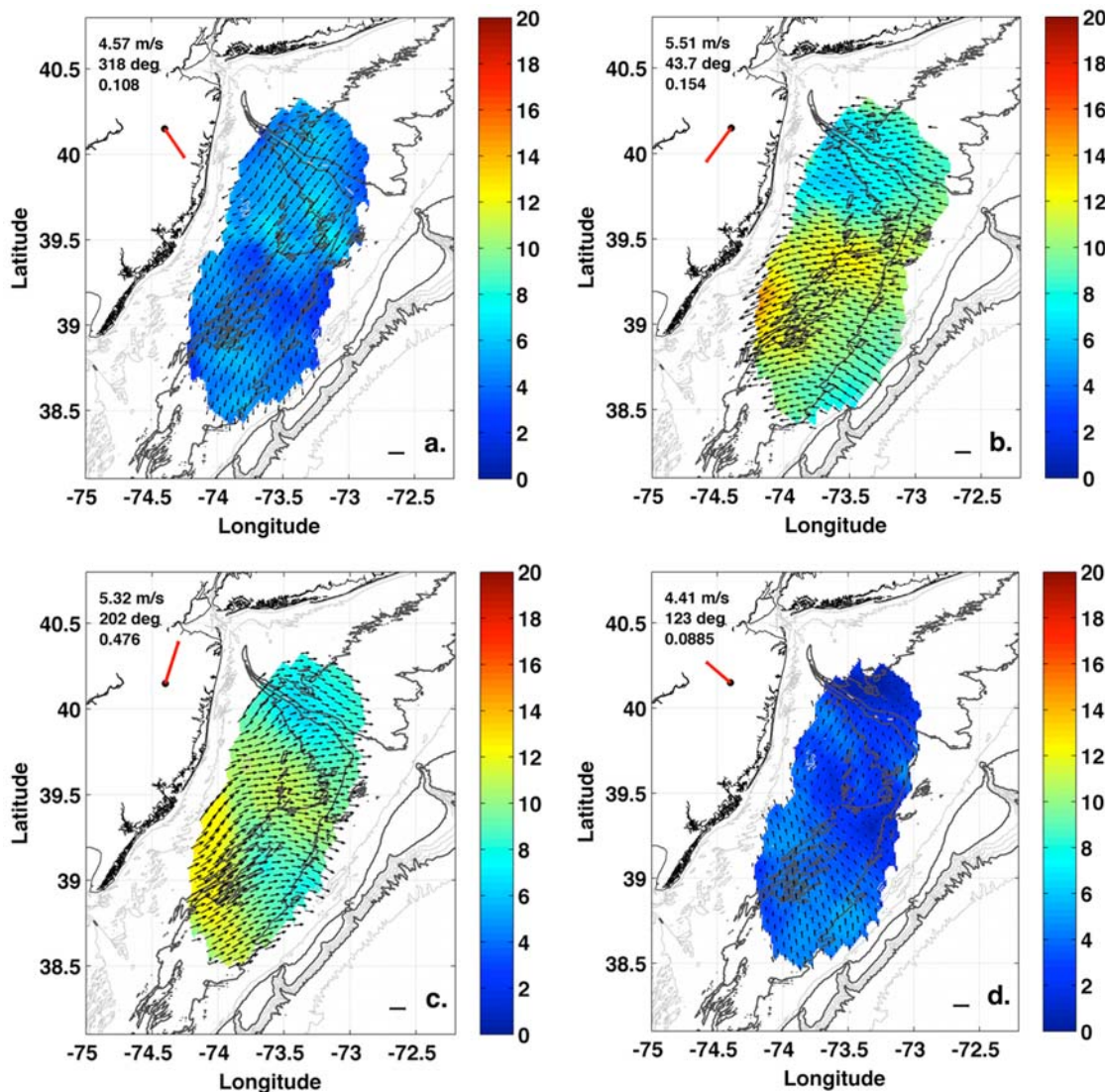


**Figure 11.** Summer mean current based on wind (cm/s): (a) northwest winds, (b) northeast winds, (c) southwest winds, and (d) southeast winds.

are significant contributors during the autumn, each account for 25, 23, and 24% of the total winds, respectively. The response of the shelf flow under NW winds is offshore and down shelf with a flow velocity of 8 to 12 cm/s south of the HSV (Figure 12a). Under SW winds the flow is offshore and up shelf, similar to the summer scenario but more intense with flows of 8 to 16 cm/s (Figure 12c). NE winds generate the most intense flow, mostly down shelf and onshore with velocities in excess of 14 cm/s for nearly the entire shelf south of the HSV with peak currents of over 20 cm/s near the Endurance Line (Figure 12b). Near the HSV, the flow is 6 to 10 cm/s. Lastly, under the onshore SE winds, the flow is weakly inshore and up shelf with a speed of 2 to 6 cm/s (Figure 12d).

[36] The response of the surface currents to the different wind forcing regimes show clear seasonal differences. The surface flow is to the right of the wind during the summer stratified season and largely in the direction of the wind during the winter mixed season. The spatial maps exhibit along-shelf variability and weak cross-shelf variability.

Flow near the Hudson Shelf Valley has a persistently weaker response to wind forcing compared to regions down shelf to the south. SW winds are most common for summer, and NW winds are most common for winter. All three major wind directions (SW, NW and NE) are significant during the transition seasons of spring and autumn. During the transition seasons, NE winds in particular generate strong down shelf and onshore flow, the most energetic surface current response to wind forcing observed on the New Jersey shelf.

#### 4.5. Wind Current Correlation

[37] The 2-D maps of surface flow from section 4.4 show that surface currents have a strong seasonal variability in response to wind forcing. This is consistent with modeling results showing the wind-driven MAB shelf flow is strongly dependent on the stratification [Keen and Glenn, 1994]. The structure of the surface and bottom boundary layers determine the vertical mixing of momentum, which is reflected observationally in the seasonal differences in the wind-current correlation angle. Weak winds and strong stratifi-

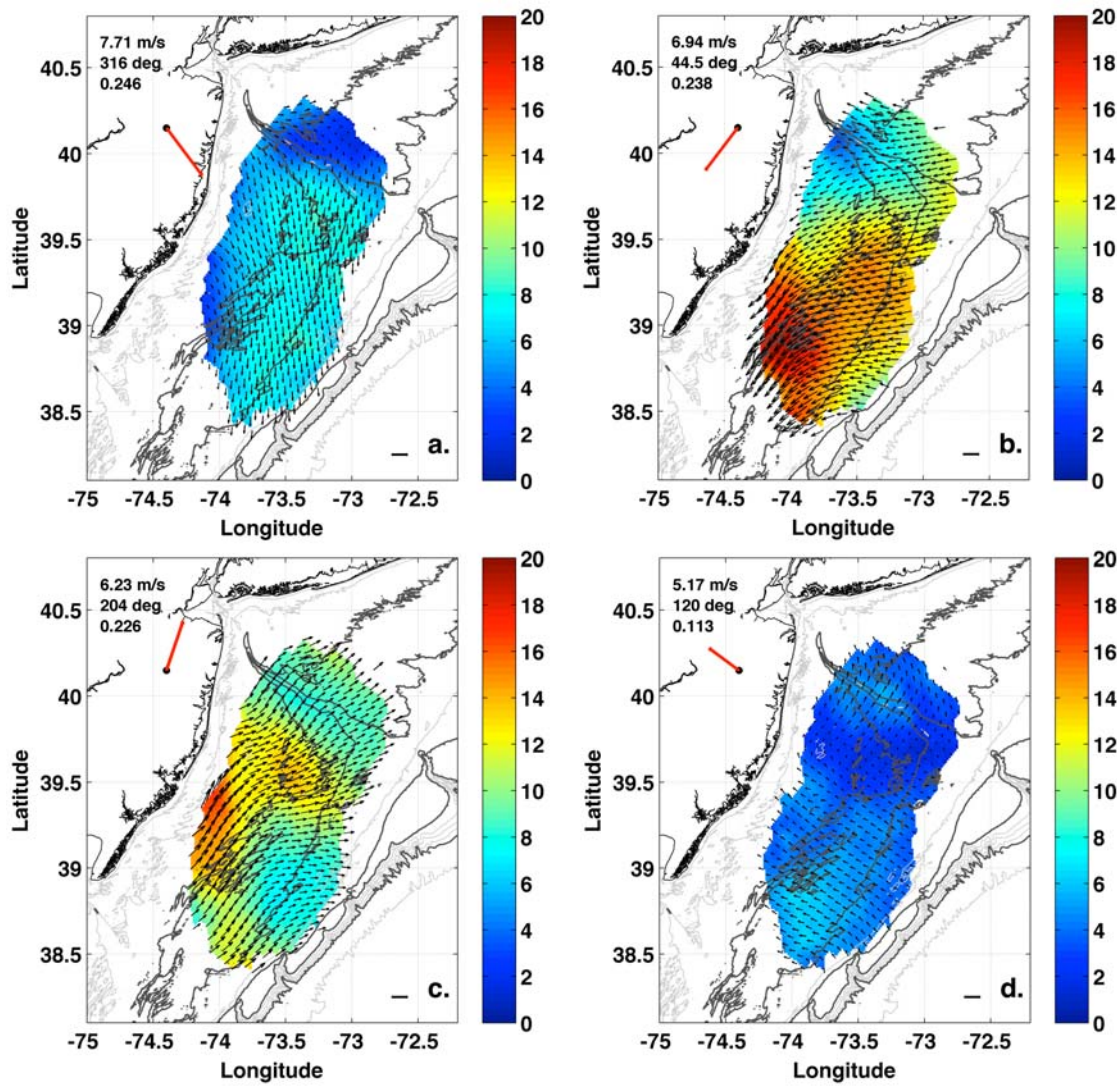


**Figure 12.** Autumn mean current based on wind (cm/s): (a) northwest winds, (b) northeast winds, (c) southwest winds, and (d) southeast winds.

cation (i.e., summer) result in separate surface and bottom layers across the shelf except at the coastal upwelling zone [Keen and Glenn, 1994]. The strong summer stratification tends to constrain the surface mixed layer to the upper 10–12 m, above the season pycnocline [Castelao et al., 2008b]. On the other hand, strong winds and moderate stratification (i.e., spring and autumn) can result in interacting boundary layers at the inner shelf [Glenn et al., 2008] and separate boundary layers over the outer shelf. Finally strong winds and weak stratification (winter) can result in interacting boundary layers across the entire shelf. One can estimate the depth of the surface Ekman layer [Csanady, 1976; Lentz, 2001] for an unstratified water column

$$\delta_s = \frac{\kappa}{f} \sqrt{\frac{\tau^s}{\rho}},$$

where  $u^* = \sqrt{\frac{\tau^s}{\rho}}$  is the shear velocity and  $\kappa = 0.4$  is von Kármán constant. Let  $f = 9 \times 10^{-5} \text{ s}^{-1}$  at latitude 39 N, and assume  $\tau = 0.1 \text{ N/m}^2$  (corresponding to 8 m/s wind at

5 meters above sea level), the surface Ekman layer depth is 43 m. If the wind stress increases to  $0.35 \text{ N/m}^2$ , as was occasionally seen on the New Jersey Shelf during the winter, the estimated surface Ekman layer would extend over 80 m. The bottom mixed layer typically has a height of less than 10 m during the stratified season but can also exceed 20 m on the MAB [Perlin et al., 2005; Lentz and Trowbridge, 1991; Glenn et al., 2008]. Solutions to the classic Ekman problem using different vertical eddy viscosities exhibit significant differences in the wind-current angle depending on

**Table 3.** Relative Variability of Detided CODAR Currents: RMS/Mean

	Summer	Winter	Spring	Autumn	All Seasons
All Directions	4.9	2.6	3.0	3.0	3.3
NW	1.9	1.4	1.4	1.6	1.6
NE	1.3	0.9	0.9	1.1	1.1
SW	1.7	1.7	1.8	1.8	1.8
SE	6.8	1.8	3.7	3.0	3.5

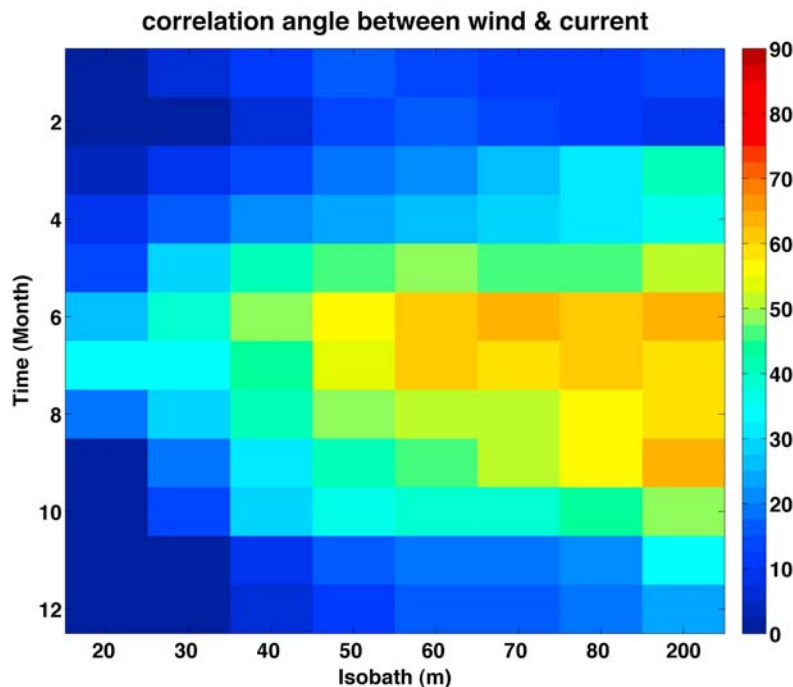


**Figure 13.** Correlation angle between wind and current along a cross-shelf transect just south of the Tuckerton Endurance Line (2002–2007).

the structure of the vertical eddy viscosity [Ekman, 1905; Madsen, 1977; Trowbridge and Lentz, 1991].

[38] It is therefore worthwhile to quantify the wind-current correlation as a function of time and space over the New Jersey Shelf. A small correlation angle would be consistent with an eddy viscosity profile of a water column with interacting boundary layers and a large angle would be consistent with a shallow surface Ekman layer and separate boundary layers. The monthly climatology of the complex cross correlation between lowpassed wind velocity and subtidal surface current velocity are calculated for eight cross-shelf stations just south of the Tuckerton Endurance Line using the 6 year CODAR data set and the NOAA wind data set from NDBC buoy 44009 (Figure 13). For this analysis, the low-wind background mean is removed from the surface current velocities. The color of each pixel indicates the angle of the complex correlation between wind and current. A correlation angle of zero (blue) signifies flow exactly in the direction of the wind and a correlation angle of 90 (red) signifies perpendicular flow to the right of the wind. The magnitude of the complex correlations range between 0.5 and 0.8 with the lower values seen at the outermost station near the 200 m isobath for this set of eight stations. For the New Jersey Shelf, the angle between the wind and the surface currents is larger during the stratified summer ( $>45^\circ$ ) and smaller during the unstratified winter ( $<20^\circ$ ) (Figure 13). In particular, during the summer months of June–August, the mid to outer shelf stations (deeper than the 50 m isobath) show a correlation angle of 60 to 70° while the same stations during the winter months December–February show a correlation angle of 10 to 20°. The inshore stations also show a seasonal difference but with less variability. At the inner most station on the 20 m isobath, for example, the wind-current correlation angle is less than 20° for most months of

the year except during the summer months when the angle increases to 35° in July. Simple Ekman theory predicts a maximum deflection angle of 45° between the wind and surface current when the vertical eddy viscosity is constant [Ekman, 1905]. The fact that correlation angles of greater than 45° are observed suggests that the non-Ekman component of the background down-shelf flow is not completely removed. Processes such as the interaction of the wind and the shelf-slope frontal jet could be a contributing factor. The correlation angle increases from the inner shelf to the midshelf near the 50 m isobath, and beyond that there is little cross-shelf variation. The transition seasons are more dynamic in nature. At each cross-shelf location, the wind-current correlation angles change rapidly during spring (increasing from April to May) and autumn (decreasing from October to November). These results suggest that the seasonal change in stratification exerts a strong influence on the response of surface flow to wind forcing on the New Jersey Shelf.

[39] To visualize the effect of wind-driven circulation in the context of along-shelf and cross-shelf transport, wind-current cross correlations along the natural geographic axes of the shelf are also calculated (Figure 14). The along-shore and cross-shore axes on the New Jersey Shelf are rotated 35° clockwise from true north. The cross correlation between the winds and currents are calculated for the along- and cross-shore wind and along- and cross-shelf currents for each month of the year along the same cross-shelf transect south of the Endurance Line noted earlier. The along-shore winds are correlated with along-shelf currents for all months of the year shoreward of the 40 m isobath (Figure 14a). The shallow inner shelf has an unstratified water column most months of the year. The overlapping bottom and surface Ekman layers would cause wind driven flow to be in the direction of the

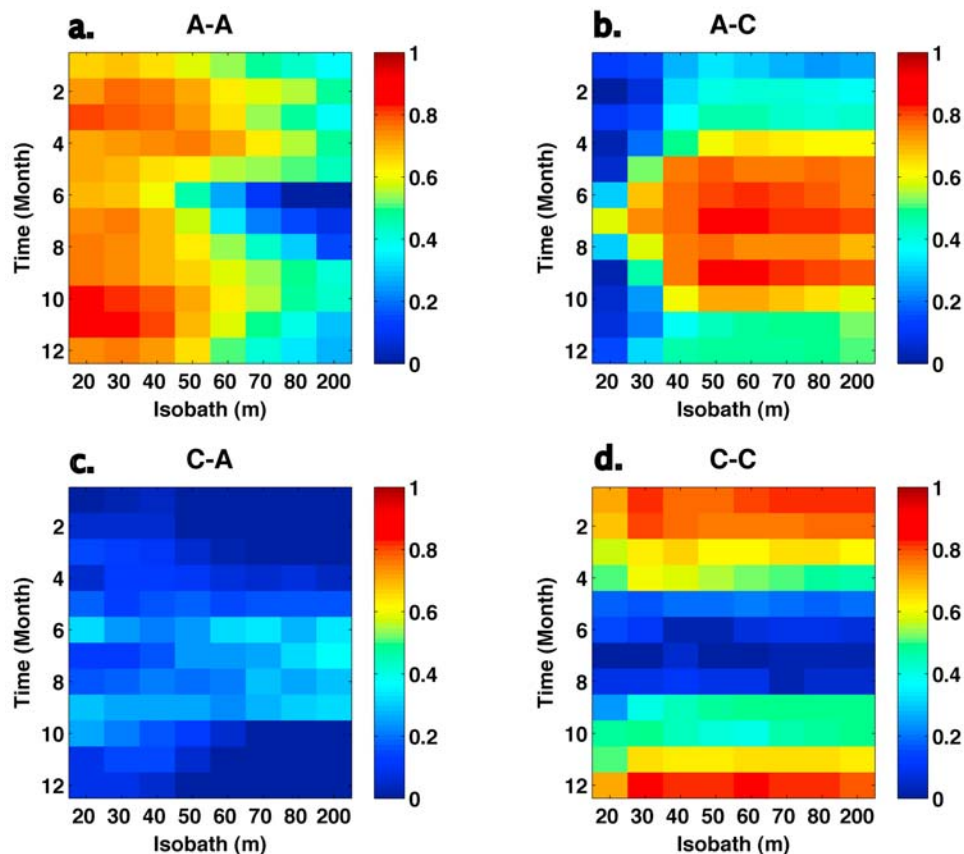


**Figure 14.** Cross correlation along geographic axes between wind and current (2002–2007): (a) along-shore winds and along-shelf current, (b) along-shore winds and cross-shelf current, (c) cross-shore winds and along-shelf current, and (d) cross-shore winds and cross-shelf current.

wind. The winds and currents are especially well correlated with each other ( $>0.7$ ) shoreward of the 50 m isobath during the spring and autumn months (Figure 14a). This could be due to the frequent occurrence of energetic along-shelf wind during the transition seasons which tend to drive along-shelf, down-shelf flow. Offshore of the 50 m isobath, the correlation decreases between the along-shore winds and the along-shelf currents. During the summer months of June, July, and August, the correlation is less than 0.3, indicating the along-shore wind is not a significant factor driving along-shelf flow at the outer shelf.

[40] The along-shelf wind is highly correlated with cross-shelf current at the mid to outer shelf from late spring to early autumn with a correlation coefficient of  $>0.8$  from May to September (Figure 14b). A linear fit between the summer along-shore winds and cross-shelf flow at the 60 m isobath is shown in Figure 15a. The slope for the summer fit is 0.0067 and it has a  $R^2$  of 0.59. This is consistent with the observations of upwelling favorable wind from the SW driving surface flow cross shelf (Figure 11c). Using a subset of the surface current data from 2003 to 2004, [Dzwonkowski *et al.*, 2009b] also finds strong summertime correlations between along-shore winds and the cross-shelf currents. Coastal upwelling due to along-shore winds on the shelf results in the offshore transport of the surface layer seaward of the upwelling region. Shoreward of the 30 m isobath, the correlation is weak, likely due to contributing factors within

the coastal upwelling zone [Glenn *et al.*, 2004]. During the unstratified periods there is a relatively weak correlation between the along-shore wind and cross-shelf current with a correlation coefficient of  $<0.5$  for October–March. This is not surprising since we know from earlier analysis that the along-shelf wind was not dominant and that the flow is in the direction of the wind during the winter season.

[41] Cross-shelf wind and cross-shelf currents have strong correlations ( $>0.7$ ) during the late autumn and winter across the entire New Jersey Shelf (Figure 14c). Since the dominant winds during late autumn and winter are mainly cross-shore, strong cross-shelf flow is observed during these times (Figure 9a). Cross-shelf depth variation does not appear to affect the variability of the cross-shore flow offshore of the 20 m isobath. A linear fit between winter cross-shore winds and cross-shelf transport at the 60 m isobath is shown in Figure 15b. The slope for the winter fit is 0.0096 and it has a  $R^2$  of 0.50, indicating a stronger response of cross-shelf flow to winter wind forcing than summer wind forcing. During the summer stratified season, the correlation between cross-shore winds and cross-shelf current is significantly reduced due to upwelling favorable along-shore winds driving cross-shelf flow.

[42] In summary, cross-shelf flow is driven by different wind patterns during the stratified summer and unstratified winter seasons. It happens that the alongshore wind is dominant during summer and cross-shore wind is dominant

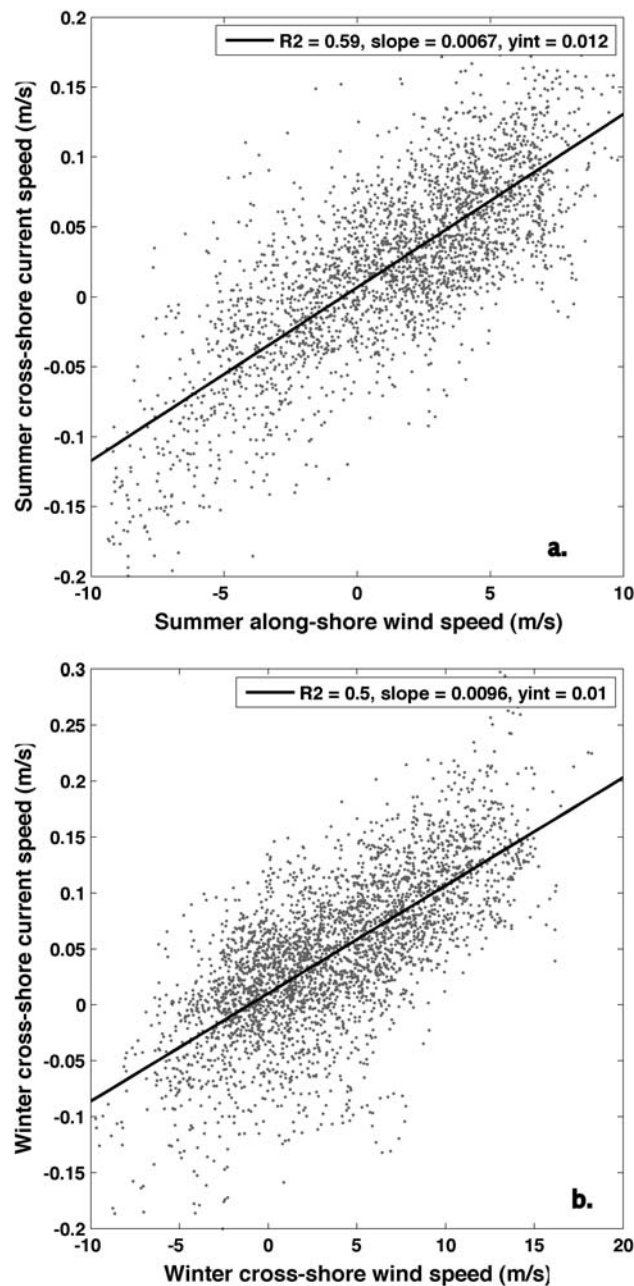


**Figure 15.** Wind-current speed correlation at a 50 m isobath site: (a) summer correlation between along-shore wind speed and cross-shore current speed and (b) winter correlation between cross-shore wind speed and cross-shore current speed.

during winter. The large wind-current correlation angle at mid to outer shelf during the summer is consistent with a shallow Ekman layer and separate boundary layers, with alongshore SW wind driving offshore flow. The small wind-current correlation angle shelf-wide during the winter is consistent with an eddy viscosity profile reflecting interacting boundary layers and cross-shore NW winds driving offshore flow. During the transition seasons of spring and autumn, boundary layer interactions are complicated by

changing stratification and frequent storms. During this time along-shelf flow is mainly driven by along-shore winds, especially at the inner to midshelf.

#### 4.6. Interannual Variability

[43] Both the magnitude and the sign of the seasonal along-shelf and cross-shelf surface flow can vary on the interannual time scale. The analysis in sections 4.3–4.5 showed that changing winds and changing water column stratification are major drivers of the seasonal and annual variability of the shelf flow. To examine the interannual variability, potential forcing functions including the Hudson River discharge (Figure 16a), New Jersey statewide average air temperatures (not shown), and along-shelf and cross-shelf winds from NDBC Buoy 44009 (Figure 16b) were seasonally averaged for each year. The along-shelf and cross-shelf current response are similarly averaged at several locations across the shelf. At each site, current vectors within a 10 km radius are averaged for each time step before being seasonally averaged. The 10 km radius was chosen to be consistent with the averaging radius used to construct CODAR vector field. Selected seasonal time series at the inner shelf (39.4 N, 73.9 W) and the outer shelf (38.95 N, 73.3 W) sites along the Tuckerton Endurance Line [*Castelao et al.*, 2008b], as well as a midshelf (39.5N, 73.3W) location to the north of the line are plotted in Figures 16c and 16d. The inner shelf site is located on the 30 m isobath near the inshore edge of the coverage area. The midshelf site is located right over the FTS near the 40 m isobath. The outer shelf site is located in between the 60 and 70 m isobaths, inshore of the shelf-slope frontal jet. The sites are chosen to highlight the interannual variability of cross-shelf flow differences.

[44] Both the summer stratified season (red) as well as the winter mixed season (blue) are characterized by consistently offshore flow across the entire shelf with low interannual variability (Figures 16c–16e, solid lines). Despite the large injection of freshwater by the Hudson River during the summer of 2006, the shelf circulation as indicated by the time series in Figure 16 is similar to the other years. For the spring (green), the cross-shelf flow also is usually offshore except for 2003. The anomalous spring of 2003 exhibited colder air temperatures (not shown), higher river discharge, and strong alongshore winds from the NE. It is the only spring with a strong onshore wind (green lines, Figure 16b), and it is the only spring in which a reversal of the cross-shelf flow to onshore at the mid and outer shelf is observed. Cross-shelf flow during autumn (purple) is largest at midshelf and is offshore, with fluctuating weak flows observed at the inshore and offshore sites.

[45] For the alongshore flow during the summer, despite the consistent upwelling favorable winds, the current is usually down shelf at the mid to outer shelf (Figures 16d and 16e, red dashed line). The only flow reversal occurs in 2003 at the midshelf when the summer upwelling wind is strongest (Figure 16b, red dashed line). In contrast to the mid and outer shelf, the summer inner shelf current oscillates around zero (Figure 16c), possibly due to the nearly equal influences of the wind-driven, up-shelf transport and the diminishing shoreward effect of the large-scale along-shelf pressure gradient. In winter, the pattern of alongshore currents on the inner shelf (Figure 16c, blue dashed line) is highly correlated with the pattern of alongshore winds

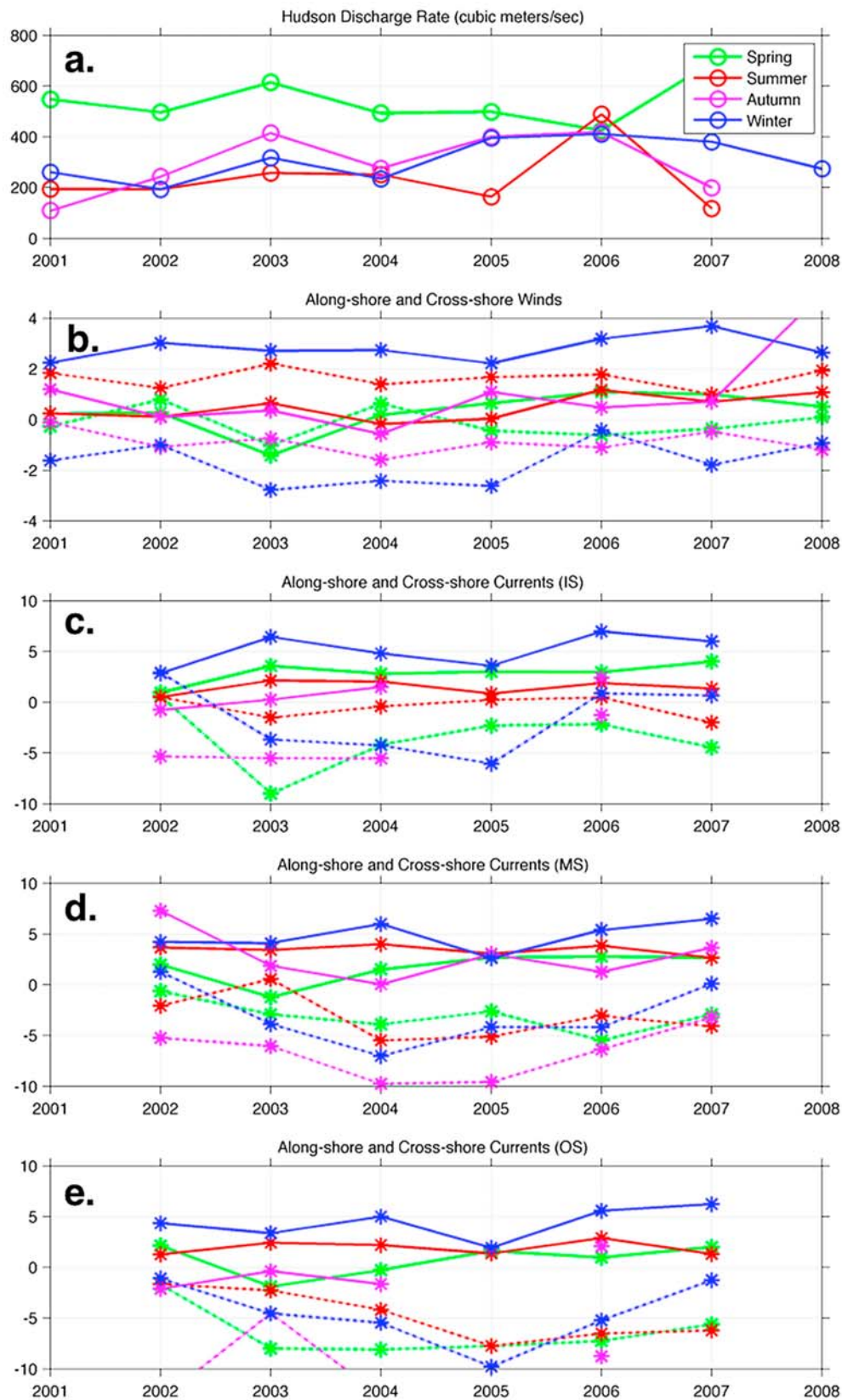


**Figure 16.** (a) Seasonal time series of Hudson River discharge; (b) along-shelf and cross-shelf winds; and mean along-shelf and cross-shelf surface current at the (c) inner shelf, (d) midshelf, and (e) outer shelf. Solid lines are cross-shore (positive is offshore), and dashed lines are along-shore (positive is up shelf). Red is summer, blue is winter, green is spring, and purple is autumn.

**Table 4.** Cross-Shelf Drifter Time, Speed, and Fraction Reaching 60 m Isobath<sup>a</sup>

	Jun 2006	Sep 2006	Dec 2006	Mar 2007	Distance to 60 m
<i>Drifter Time</i>					
Site N	13.6	30.7	23.9	36.1	97
Site C	13.3	20.5	17.4	24.8	82
Site S	12.9	13.1	14.9	27.6	67
<i>Drifter Speed</i>					
Site N	49.9	22.1	28.4	18.8	97
Site C	43.2	28.0	33.0	23.1	82
Site S	36.4	35.8	31.5	21.4	67
<i>Fraction Reaching 60 m</i>					
Site N	0.27	0.09	0.73	0.39	97
Site C	0.68	0.17	0.99	0.71	82
Site S	0.77	0.25	1.00	0.45	67

<sup>a</sup>Time in days, speed in km/week, and distance in km.

(Figure 16b, blue dashed line). A reversal in the winter alongshore current to up shelf at the inner shelf location in 2002, 2006 and 2007 is observed when the alongshore NE winter winds weaken below 2 m/s. At the midshelf, the alongshore current reverses to up shelf in only winter 2002 and summer 2003. Spring along-shelf flow is persistently down shelf. The anomalous 2003 experienced the strongest down-shelf flow at the inner shelf site, consistent with a buoyant river plume driven by high river discharge, the only onshore spring winds, and strong downwelling favorable winds from the NE (Figure 16c). Along-shelf flow is strongest and down shelf in autumn, especially at the midshelf where 2004 and 2005 were especially intense.

#### 4.7. Transport and Residence Time

[46] Understanding the transport pathways and residence time of material is important for addressing many biogeochemical questions on continental shelves. The MAB is highly productive and its biological activity exhibits strong seasonal cycles [Schofield *et al.*, 2008]. Analysis of Eulerian surface current data in sections 4.3–4.5 have shown that circulation on the shelf also has strong seasonal cycles driven by seasonal wind forcing and changing stratification. Given the potential influence of shelf circulation on biogeochemical activities, we want to examine the potential transport pathways and estimate the residence time on the New Jersey Shelf from a Lagrangian perspective. The large spatial coverage area of the CODAR fields, the high temporal resolution, and the long observation duration allow us to capture the advective state of the ocean and use it in a numerical Lagrangian drifter study. To visualize the transport pathways, virtual drifters are deployed in the CODAR fields at various locations on the New Jersey Shelf. The Lagrangian virtual drifter study focuses on the long-range CODAR data from June 2006 to May 2007. This time period has excellent data coverage and as the previous interannual study indicates, does not exhibit anomalous seasonal circulation patterns compared to the other years.

[47] The effect of dispersion in the virtual drifter advection scheme associated the instrument uncertainty and the subgrid-scale variability is estimated using a Markovian random flight model [Griffa, 1996]. Prior applications of this type of drifter dispersion model include the U. S. Coast Guard Search and Rescue (SAR) comparison study of CODAR virtual drifters and actual Self-Locating Datum

Marker Buoys (SLDMB) [Ullman *et al.*, 2006]. The random flight method they used provided search areas that enclose the real drifter approximately 90% of the time in this same CODAR current field. A set of best fit parameters for the U and V components of the turbulent velocity dispersion on the New Jersey Shelf are derived by minimizing the least squared difference between the actual drifters and the virtual drifters. The same methodology and the same set of best fit turbulence parameters from Table 2 of Ullman *et al.* [2006] are used to estimate the combined instrument uncertainty and the subgrid-scale dispersion. The U component of the velocity dispersion  $\sigma_u$  is 11 cm/s and the V component  $\sigma_v$  is 12 cm/s, with the turbulent time scales  $T_u = 3.3$  hours and  $T_v = 3.1$  hours.

[48] The integration of the drifter velocities is formulated using a first-order scheme. The error associated with the first-order integration is the highest for a circular flow field such as that of an eddy. Persistent eddy fields on the shelf, however, are rare. We estimate the advective error for a typical situation and compare with the dispersion error associated with uncertainty in the velocity field. Assuming a current speed of 30 cm/s, a radius of curvature of 50 km as discussed before, and an integration step of 3 hours, the maximum advective error from using a first-order integration scheme for each time step is 0.1 km. On the other hand, assuming a velocity dispersion of 11 cm/s, the random distance per time step of integration (3 hours) is 1.2 km. The numerical error introduced by using a first-order advection scheme is an order of magnitude smaller than the uncertainty associated with subgrid-scale variability for typical flow conditions, justifying its usage.

[49] Two sets of virtual drifter experiments are performed. The first set deploys virtual drifters at three inshore sites to determine the cross-shelf transport pathways and residence times during all four seasons. The amount of time it takes each of the drifters to reach the 60 m isobath is calculated. The three deployment sites are chosen to capture the cross-shelf transport for different parts of the New Jersey Shelf while maximizing the drifters exposure to the high data coverage areas. These locations are consistent with regions of offshore flow seen in the HF Radar data between 2003 and 2004 [Dzwonkowski *et al.*, 2009a]. The northern release site (N) is located on the HSV at (73.66 W, 40.18 N), the central release site (C) is located 20 km offshore of Loveladies, New Jersey (73.85 W, 39.70 N), and the southern release site (S) is situated 30 km offshore of Tuckerton, New Jersey (74.00 W, 39.30 N). The sites are located 97 km, 82 km and 67 km from the 60 m isobath, respectively. One drifter is deployed every 3 hours at each location for 30 days and is then allowed to drift for up to 90 days. Occasional missing CODAR grid points are filled in with the mean current from each 90 day interval. Drifters are stopped once they reach the boundary of the CODAR coverage or the 60 m isobath line. The mean travel time, the cross-shore speed, and the fraction of drifters reaching the 60 m isobath from their release locations are listed in Table 4. Example transport pathways for drifters released at Site C, offshore of Loveladies, are shown for the summer 2006 (Figure 17d) and the winter 2006 (Figure 17a).

[50] For the study period from June 2006 to May 2007, drifters deployed at the inner shelf that reached the outer shelf 60 m isobath took 2 to 5 weeks, traveling at speeds of

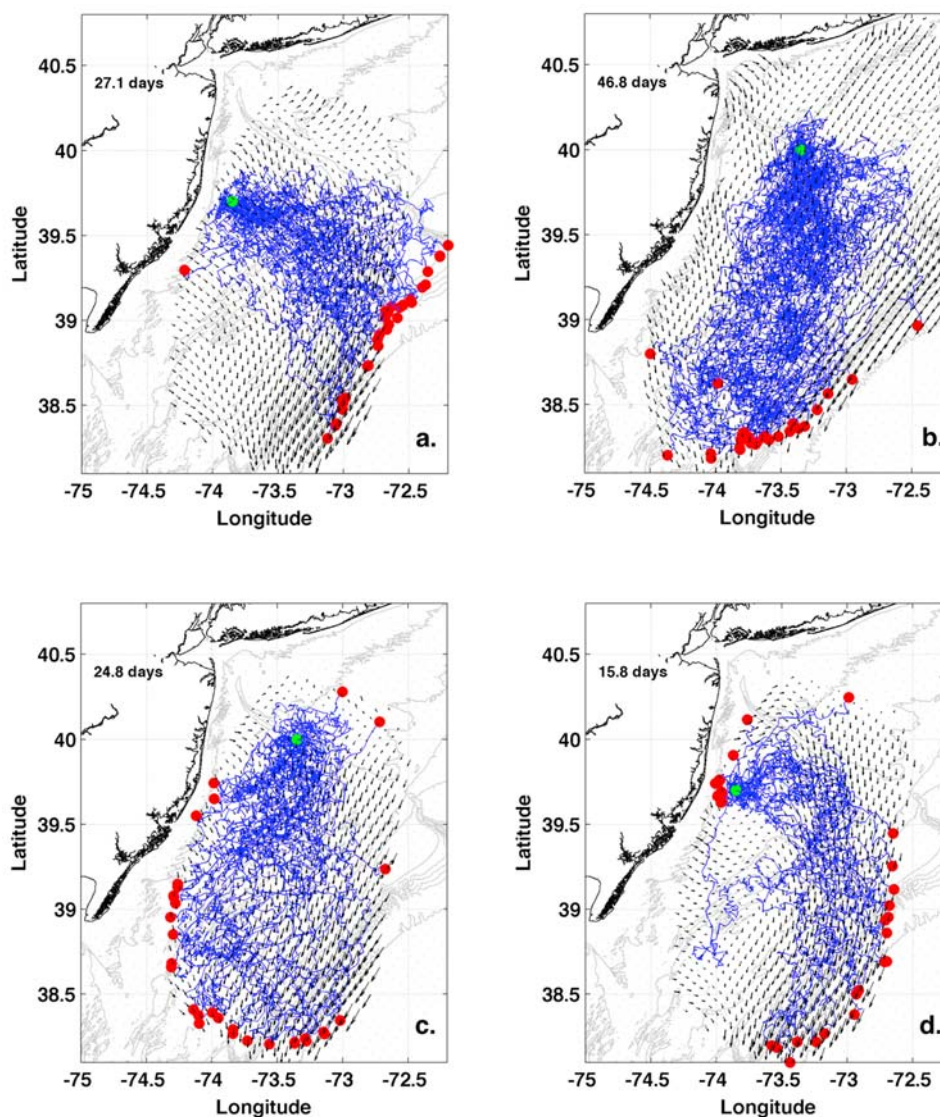


**Figure 17.** Virtual drifter transport study; green dot is deployment location, and red dots are end locations. Mean transport times are printed. (a) Winter (December 2006), (b) spring (March 2007), (c) autumn (September 2006), and (d) summer (June 2006).

19 to 50 km/week. Summer experienced the fastest cross-shelf flow and spring exhibited the slowest (Table 4). Summertime upwelling favorable winds and the winter offshore winds result in the persistent offshore advection of the surface drifters. The majority of the drifters deployed during the stratified summer and well-mixed winter reach the 60 m isobath boundary. During the transition seasons of spring and autumn, a significant fraction of the drifters do not reach the 60 m isobath, instead they exit through the inshore/down-shelf pathway. A particularly interesting feature of summer drifters is that they are often advected up shelf along the inner shelf before moving cross-shelf at the midshelf and eventually veer down shelf near the shelf break. This inverted U-shaped pattern south of the HSV (Figure 17d) is a persistent circulation feature of summer 2006. The average cross-shelf speed of the drifters is 43 km/week, significantly faster than the average winter cross-shelf speed of 31 km/week. The average cross-shelf speed for the

minor fraction of drifters released in spring 2007 and autumn 2006 that do make it across to the 60 m isobath are 21 km/week and 29 km/week, respectively. There is large scatter in the actual traversal time of individual drifters. Some of the virtual drifters can cross the shelf in a week whereas others can take over a month. The summer drifter paths show less spatial scatter compared to the paths of the winter drifters.

[51] The second set of drifter experiments focuses on illustrating the residence time and transport pathways during the transition seasons of spring and autumn. Spring and autumn mean fields are generally dominated by along-shelf flow on the New Jersey Shelf. Drifters are released at a site situated over the HSV (73.35 W, 40.00 N) for two seasons at the beginning of spring (March 2007; Figure 17b) and the beginning of autumn (September 2006; Figure 17c). The drifter deployment location is chosen to maximize their data exposure in the along-shelf direction. The spring drifters take an average of a month and half to travel the length of

the New Jersey Shelf with relatively little scatter despite the month long release schedule (Figure 17b). The average along-shelf velocity for the spring drifters is approximately 25 km/week. Recall that NE winds become more frequent during the spring time. When the wind is from the NE, the surface flow is predominantly down shelf and alongshore. For autumn, winds from the SW, NW and NE all occur about the same percentage of time although NE winds generate the most energetic flows. While the different wind conditions of autumn likely cause the drifters to follow more scattered paths, the drifters still exhibit a clear alongshore down-shelf movement (Figure 17c). Drifters deployed during the month of September 2006, for example, show a variety of down-shelf transport pathways, some exit the study region at the inner shelf, some head down at midshelf while others are exported toward the shelf break. Despite the more scattered drift paths, however, the autumn drifters move at a significantly faster speed down the shelf, taking approximately 3–4 weeks at an average speed of 44 km/week, nearly twice as fast compared to the spring season. On average the along-shelf transport time scale for the transition seasons is the same as the cross-shelf transport time scale for the stratified and mixed seasons on the New Jersey Shelf.

## 5. Discussion

[52] Large-scale background flow, local shelf topography, changes in stratification and wind forcing influence the spatial and temporal transport patterns on the New Jersey shelf. The surface flow under various wind and stratification regimes display both coherent large-scale patterns as well as small-scale variability. Shelf-scale wind forcing and background flow determines the large-scale patterns of along-shelf or cross-shelf transport while local topography modulates the direction and magnitude of the flow near the HSV/FTS region. The different forcing mechanisms come together such that during the transition seasons of spring and autumn, the surface transport on the shelf is primarily alongshore and down shelf while during the stratified summer and mixed winter seasons the surface transport on the shelf is primarily cross-shelf and offshore. Through the annual cycle the location of the down-shelf transport shifts. During the transition seasons of the autumn and spring down-shelf flow stretches across the entire shelf. During the winter and summer seasons, the down-shelf flow is pushed offshore along the shelf break, fed by the flow of the inner and midshelf.

[53] Such seasonal shift in circulation pattern could affect the rate of volume transport on the shelf. Previous studies of MAB watermasses showed that the volume of the shelf water can vary seasonally with a magnitude on the order of the mean volume [Manning, 1991; Mountain, 2003]. Shelf water, defined to be water with salinity less than 34, reaches a maximum southwestward extent during the summer and retreats to a minimum volume during the winter [Mountain, 2003]. We observed that the seasons of maximum and minimum shelf water volume are characterized by mainly cross-shelf transport, whereas seasons with the maximum change in the shelf water volume are characterized by mainly along-shelf transport. The seasonal cycle of shelf water volume was attributed to a change in the influx of the Scotian Shelf Water [Manning, 1991]. A study by [Lentz, 2008b]

using moored current meter data from the central MAB found that the magnitude of the seasonal variability of the along-shelf depth-averaged flow to be comparable to the mean, on the order of 4–6 cm/s. He attributed such variability to wind forcing, river discharge and the seasonal cycle of the cross-shelf density gradient over the shelf. We note that during the transition seasons of spring and autumn, when the maximum change in the shelf water volume in the central MAB occurs, alongshore NE winds also become more common (Figures 10b and 12b) and they appear to drive strong along-shelf surface flow and transport (Figures 8b, 8c, 17b, and 17c). During the summer stratified season and the winter mixed season, the New Jersey Shelf switches from an along-shelf flow regime to a cross-shelf flow regime. The cross-shelf surface flow, evident in both the seasonal mean fields (Figures 8a and 8d) and the Lagrangian drifter maps (Figures 17a and 17d), suggests a surface export from the shelf which must be balanced by a return onshore flow at depth as is the case with the inner shelf [Fewings *et al.*, 2008]. Such cross-shelf circulation patterns would imply that cross-shore shelf-slope exchange is enhanced during the winter and summer periods.

[54] Over the interannual time scale, the seasonal mean along-shelf and cross-shelf flow for each year closely follows the 6 year mean from 2002 to 2007. No long-term trends in the transport were observed at various cross-shelf locations. However, there are anomalous seasons for some of the years. For example, the spring of 2003 had higher Hudson River discharge, colder air temperature, more frequent NE winds and bigger down-shelf, inner shelf flow than the other years. This was a particularly stormy spring that could have delayed the onset of seasonal stratification and the timing of the spring bloom. The summer of 2006 had very high seasonal Hudson River discharge but the flow velocity at the inner, mid and outer shelf are not significantly different from the other years. Shifts in the seasonal wind pattern over the longer time scale, such as those associated with the Atlantic Multi-decadal Oscillation (AMO) [Delworth and Mann, 2000; Kerr, 2000], could affect the seasonal shelf circulation as well as the biological response. A shift in the phase of the AMO from negative to positive took place in the mid-1990s [Schofield *et al.*, 2008]. Analysis of the decadal pattern in wind variability and changes in biological productivity have shown that the negative phase of the AMO is associated with weaker winter winds and higher productivity whereas positive phase of the AMO is associated with stronger winter winds and lower productivity [Schofield *et al.*, 2008]. Cross-shelf flow is significantly correlated with cross-shore and along-shore wind forcing at the midshelf during winter and summer, respectively (Figure 14). We therefore expect that during the years when the seasonal winter wind forcing is weak, there will be a weaker cross-shelf surface transport over the New Jersey Shelf. On the decadal time scale, we expect to see stronger wintertime cross-shelf transport during the present positive phase of the AMO and weaker wintertime cross-shelf transport during the negative phase of the AMO.

[55] The different flow patterns for each of the seasons on the New Jersey Shelf are likely to have important implications for physical transport-dependent biological processes such as shelf primary production [Schofield *et al.*, 2008; Y. Xu *et al.*, manuscript in preparation, 2009] and recruitment

dynamics of key shelf fish species [Nelson *et al.*, 1977; Werner *et al.*, 1997; Hare *et al.*, 1999; Quinlan *et al.*, 1999].

## 6. Summary

[56] Here we study the spatial and temporal variability of the surface flow on the New Jersey Shelf over a six year period from 2002 to 2007. The mean surface flow on the New Jersey Shelf is equatorward and offshore toward the south. The flow is significantly affected by bottom topography, stratification and wind forcing on the monthly to annual time scales. A band of higher-velocity cross-shelf flow exists in the mean field just south of the Hudson Shelf Valley, indicating that the valley exerts a dynamical influence on the surface flow at the longest time scales. Furthermore, the HSV acts as a dynamical boundary between flow to the north and flow to the south. Divergent flow is observed over the HSV and to the north whereas convergent flow is observed just to the south. The shelf undergoes large changes in stratification from well mixed during the winter to highly stratified during the summer. The response of the surface flow is characterized for the dominant wind conditions of the different seasons. The angle between wind stress and surface current is larger when the water column is more stratified and it exceeds Ekman theory at the mid to outer shelf. The angle is small ( $<25^\circ$ ) when the water column is well mixed. On the seasonal time scale, the surface flow oscillates between being along-shelf dominated during the transition seasons of spring and autumn and cross-shelf dominated during the stratified and well-mixed seasons of winter and summer. Cross correlation of winds and currents along a cross-shelf transect south of the Tuckerton Endurance Line show that the winter cross-shelf flow is highly correlated with cross-shore winds dominated by the NW winds, and the summer cross-shelf flow is highly correlated with along-shore winds dominated by the SW winds. Flows during the transition seasons are mainly along-shelf and they are correlated with the along-shore NE winds. From a Lagrangian perspective, the summer and winter drifters move predominantly cross-shelf. They make their way across the shelf over the period of 2 to 5 weeks. Spring drifters travel mainly alongshore and take 4–7 weeks to travel the along-shore distance of the New Jersey Shelf. Autumn drifters move and scatter on the shelf rapidly due to the energetic surface flow often driven by storms; their paths can scatter over the whole shelf and the drifters can exit the New Jersey Shelf via a variety of pathways at the inner, mid and outer shelf in a month or less. Physical transport can affect shelf biology over temporal scales from days to decades. Changes in wind strength associated with decadal shift in climate pattern can drive changes in the cross-shelf and along-shelf transport which can potentially affect shelf primary production and recruitment dynamics of key MAB fish species.

[57] **Acknowledgments.** The authors are thankful for helpful comments and suggestions from Renato Castelao, Robert Chant, Glen Gawarkiewicz, Elias Hunter, John Manderson, Patricia Ramey, Oscar Schofield, and John Wilkin. The authors would especially like to thank the RUCOOL operational team led by Hugh Roarty who has worked extremely hard to keep the HF Radar network up and running during the long study period. The HF Radar network used in this study was supported by the Office of Naval Research (ONR), the National Oceanic and Atmospheric Administration (NOAA), the Department of Homeland

Security (DHS), the National Science Foundation (NSF), the Department of Defense (DoD), and the National Oceanographic Partnership Program (NOPP). The research was supported by the Office of Naval Research grants Shallow Water 2006 N00014-06-1-0283 and Nonlinear Internal Wave Initiative N00014-08-1-0373.

## References

- Allen, J. S. (1980), Models of wind-driven currents on the continental shelf, *Annu. Rev. Fluid Mech.*, *12*(1), 389–433, doi:10.1146/annurev.fl.12.010180.002133.
- Allen, J. S., and R. L. Smith (1981), On the dynamics of wind-driven shelf currents, *Philos. Trans. R. Soc. London Ser. A*, *302*(1472), 617–634.
- Barrick, D. E. (1971a), Theory of HF/VHF propagation across the rough sea: 1. The effective surface impedance for a slightly rough highly conducting medium at grazing incidence, *Radio Sci.*, *6*, 517–526.
- Barrick, D. E. (1971b), Theory of HF/VHF propagation across the rough sea: 2. Application to HF/VHF propagation above the sea, *Radio Sci.*, *6*, 527–533.
- Beardsley, R. C., and W. C. Boicourt (1981), On estuarine and continental-shelf circulation in the Middle Atlantic Bight, in *Evolution of Physical Oceanography: Scientific Surveys in Honor of Henry Stommel*, edited by B. A. Warren and C. Wunsch, pp. 198–235, MIT Press, Cambridge, Mass.
- Beardsley, R. C., and C. D. Winant (1979), On the mean circulation in the Mid-Atlantic Bight, *J. Phys. Oceanogr.*, *9*(3), 612–619.
- Beardsley, R. C., W. C. Boicourt, and D. Hanson (1976), Physical oceanography of the Mid-Atlantic Bight, *Spec. Symp. Am. Soc. Limnol. Oceanogr.*, *2*, 20–34.
- Beardsley, R. C., D. C. Chapman, K. H. Brink, S. R. Ramp, and R. Schlitz (1985), The Nantucket Shoals Flux Experiment (NSFE79). Part I: A basic description of the current and temperature variability, *J. Phys. Oceanogr.*, *15*(6), 713–748.
- Bigelow, H. B. (1933), Studies of the waters on the continental shelf, Cape Cod to Chesapeake Bay. I. The cycle of temperature, *Pap. Phys. Oceanogr. Meteorol.*, *2*(4), 1–135.
- Bigelow, H. B., and M. Sears (1935), Studies of the waters on the continental shelf, Cape Cod to Chesapeake Bay. II. Salinity, *Pap. Phys. Oceanogr. Meteorol.*, *4*(1), 1–94.
- Biscaye, P. E., C. N. Flagg, and P. G. Falkowski (1994), The shelf edge exchange processes experiment, Seep-II: An introduction to hypotheses, results and conclusions, *Cont. Shelf Res.*, *41*(2–3), 231–252.
- Bumpus, D. F. (1973), A description of the circulation on the continental shelf of the east coast of the United States, *Prog. Oceanogr.*, *6*, 111–157.
- Byoung-Ju, C., and J. L. Wilkin (2007), The effect of wind on the dispersal of the Hudson River Plume, *J. Phys. Oceanogr.*, *37*(7), 1878–1897.
- Castelao, R., O. Schofield, S. Glenn, R. Chant, and J. Kohut (2008a), Cross-shelf transport of freshwater on the New Jersey Shelf, *J. Geophys. Res.*, *113*, C07017, doi:10.1029/2007JC004241.
- Castelao, R., S. Glenn, O. Schofield, R. Chant, J. Wilkin, and J. Kohut (2008b), Seasonal evolution of hydrographic fields in the central Middle Atlantic Bight from glider observations, *Geophys. Res. Lett.*, *35*, L03617, doi:10.1029/2007GL032335.
- Chant, R. J., S. M. Glenn, E. Hunter, J. Kohut, R. F. Chen, R. W. Houghton, J. Bosch, and O. Schofield (2008), Bulge formation of a buoyant river outflow, *J. Geophys. Res.*, *113*, C01017, doi:10.1029/2007JC004100.
- Chapman, D. C., and R. C. Beardsley (1989), On the origin of shelf water in the Middle Atlantic Bight, *J. Phys. Oceanogr.*, *19*(3), 384–391.
- Chapman, D. C., and H. C. Graber (1997), Validation of HF radar measurements, *Oceanography*, *10*, 76–79.
- Chapman, D. C., and S. J. Lentz (1994), Trapping of a coastal density front by the bottom boundary-layer, *J. Phys. Oceanogr.*, *24*(7), 1464–1479.
- Churchill, J. H., J. P. Manning, and R. C. Beardsley (2003), Slope water intrusions onto Georges Bank, *J. Geophys. Res.*, *108*(C11), 8012, doi:10.1029/2002JC001400.
- Csanady, G. T. (1976), Mean circulation in shallow seas, *J. Geophys. Res.*, *81*(6), 5389–5399.
- Delworth, T. L., and M. E. Mann (2000), Observed and simulated multidecadal variability in the Northern Hemisphere, *Clim. Dyn.*, *16*(9), 661–676, doi:10.1007/s003820000075.
- Dzwonkowski, B., J. T. Kohut, and X. H. Yan (2009a), Sub-inertial characteristics of the surface flow field over the shelf of the central Mid-Atlantic Bight, *Cont. Shelf Res.*, *29*, 1873–1886.
- Dzwonkowski, B., J. T. Kohut, and X. H. Yan (2009b), Seasonal differences in wind-driven across-shelf forcing and response relationships in the shelf surface layer of the central Mid-Atlantic Bight, *J. Geophys. Res.*, *114*, C08018, doi:10.1029/2008JC004888.
- Ekman, V. W. (1905), On the influence of the Earth's rotation on ocean current, *Ark. Mat. Astron. Fys.*, *2*, 1–53.

- Fewings, M., S. J. Lentz, and J. Fredericks (2008), Observations of cross-shelf flow driven by cross-shelf winds on the inner continental shelf, *J. Phys. Oceanogr.*, *38*(11), 2358–2378.
- Flagg, C. N., R. W. Houghton, and L. J. Pietrafesa (1994), Summertime thermocline salinity maximum intrusions in the Mid-Atlantic Bight, *Deep Sea Res. Part II*, *41*(2–3), 325–340.
- Flagg, C. N., L. J. Pietrafesa, and G. L. Weatherly (2002), Springtime hydrography of the southern Middle Atlantic Bight and the onset of seasonal stratification, *Deep Sea Res. Part II*, *49*(20), 4297–4329.
- Flagg, C. N., M. Dunn, D. P. Wang, H. T. Rossby, and R. L. Benway (2006), A study of the currents of the outer shelf and upper slope from a decade of shipboard ADCP observations in the Middle Atlantic Bight, *J. Geophys. Res.*, *111*, C06003, doi:10.1029/2005JC003116.
- Fong, D. A., and W. R. Geyer (2001), Response of a river plume during an upwelling favorable wind event, *J. Geophys. Res.*, *106*, 1067–1084.
- Garvine, R. W. (2004), The vertical structure and subtidal dynamics of the inner shelf off New Jersey, *J. Mar. Res.*, *62*(3), 337–371.
- Gawarkiewicz, G., and D. C. Chapman (1992), The role of stratification in the formation and maintenance of shelf-break fronts, *J. Phys. Oceanogr.*, *22*(7), 753–772.
- Gawarkiewicz, G., T. G. Ferdeman, T. M. Church, and G. W. Luther (1996), Shelfbreak frontal structure on the continental shelf north of Cape Hatteras, *Cont. Shelf Res.*, *16*(14), 1751–1773.
- Gawarkiewicz, G., F. Bahr, R. C. Beardsley, and K. H. Brink (2001), Interaction of a slope eddy with the shelf break front in the Middle Atlantic Bight, *J. Phys. Oceanogr.*, *31*(9), 2783–2796.
- Glenn, S., and O. Schofield (2009), Growing a distributed ocean observatory: Our view from the COOLroom, *Oceanography*, *22*(2), 112–129.
- Glenn, S., et al. (2004), Biogeochemical impact of summertime coastal upwelling on the New Jersey Shelf, *J. Geophys. Res.*, *109*, C12S02, doi:10.1029/2003JC002265.
- Glenn, S., C. Jones, M. Twardowski, L. Bowers, J. Kerfoot, J. Kohut, D. Webb, and O. Schofield (2008), Glider observations of sediment resuspension in a Middle Atlantic Bight fall transition storm, *Limnol. Oceanogr.*, *53*(5), 2180–2196.
- Gong, D., S. Glenn, R. Chant, J. Wilkin, and J. Kohut (2006), NJ Turnpike—Dynamics of the Hudson Shelf Valley, *Eos Trans. AGU*, *87*(36), Ocean Sci. Meet. Suppl., Abstract OS341-05.
- Griffa, A. (1996), Applications of stochastic particle models to oceanographic problems, in *Stochastic Modelling in Physical Oceanography*, vol. 113, edited by R. J. Adler, P. Muller, and B. Rozovskii, Birkhauser, Boston.
- Hare, J. A., J. A. Quinlan, F. E. Werner, B. O. Blanton, J. J. Govoni, R. B. Forward, L. R. Settle, and D. E. Hoss (1999), Larval transport during winter in the SABRE study area: Results of a coupled vertical larval behaviour—three-dimensional circulation model, *Fish. Oceanogr.*, *8*, 57–76.
- Hare, J. A., J. H. Churchill, R. K. Cowen, T. J. Berger, P. C. Cornillon, P. Dragos, S. M. Glenn, J. J. Govoni, and T. N. Lee (2002), Routes and rates of larval fish transport from the southeast to the northeast United States continental shelf, *Limnol. Oceanogr.*, *47*(6), 1774–1789.
- Harris, C. K., B. Butman, and P. Traykovski (2003), Winter-time circulation and sediment transport in the Hudson Shelf Valley, *Cont. Shelf Res.*, *23*(8), 801–820.
- Hunter, E., R. Chant, L. Bowers, S. Glenn, and J. Kohut (2007), Spatial and temporal variability of diurnal wind forcing in the coastal ocean, *Geophys. Res. Lett.*, *34*, L03607, doi:10.1029/2006GL028945.
- Keen, T. R., and S. M. Glenn (1994), A coupled hydrodynamic-bottom boundary layer model of Ekman flow on stratified continental shelves, *J. Phys. Oceanogr.*, *24*(8), 1732–1749.
- Keen, T. R., and S. M. Glenn (1995), A coupled hydrodynamic-bottom boundary layer model of storm and tidal flow in the Middle Atlantic Bight of North America, *J. Phys. Oceanogr.*, *25*(3), 391–406.
- Kerr, R. A. (2000), A North Atlantic climate pacemaker for the centuries, *Science*, *288*(5473), 1984–1985, doi:10.1126/science.288.5473.1984.
- Knebel, H. J., and E. C. Spiker (1977), Thickness and age of surficial sand sheet, Baltimore Canyon Trough area, *Am. Assoc. Pet. Geol. Bull.*, *61*, 861–871.
- Kohut, J. T., S. M. Glenn, and R. J. Chant (2004), Seasonal current variability on the New Jersey inner shelf, *J. Geophys. Res.*, *109*, C07S07, doi:10.1029/2003JC001963.
- Kohut, J. T., S. M. Glenn, and J. D. Paduan (2006a), Inner shelf response to Tropical Storm Floyd, *J. Geophys. Res.*, *111*, C09S91, doi:10.1029/2003JC002173.
- Kohut, J. T., H. J. Roarty, and S. M. Glenn (2006b), Characterizing observed environmental variability with HF Doppler radar surface current mappers and acoustic Doppler current profilers: Environmental variability in the coastal ocean, *IEEE J. Oceanic Eng.*, *31*(4), 876–884.
- Lentz, S. J. (2001), The influence of stratification on the wind-driven cross-shelf circulation over the North Carolina Shelf, *J. Phys. Oceanogr.*, *31*(9), 2749–2760.
- Lentz, S. J. (2003), A climatology of salty intrusions over the continental shelf from Georges Bank to Cape Hatteras, *J. Geophys. Res.*, *108*(C10), 3326, doi:10.1029/2003JC001859.
- Lentz, S. J. (2008a), Observations and a model of the mean circulation over the Middle Atlantic Bight continental shelf, *J. Phys. Oceanogr.*, *38*(6), 1203–1221.
- Lentz, S. J. (2008b), Seasonal variations in the circulation over the Middle Atlantic Bight continental shelf, *J. Phys. Oceanogr.*, *38*(7), 1486–1500.
- Lentz, S. J., and J. H. Trowbridge (1991), The bottom boundary layer over the northern California Shelf, *J. Phys. Oceanogr.*, *21*(8), 1186–1201.
- Linder, C. A., and G. Gawarkiewicz (1998), A climatology of the shelf break front in the Middle Atlantic Bight, *J. Geophys. Res.*, *103*(C9), 18,405–18,423.
- Madsen, O. S. (1977), A realistic model of the wind-induced Ekman boundary layer, *J. Phys. Oceanogr.*, *7*(2), 248–255.
- Manning, J. (1991), Middle Atlantic Bight salinity: Interannual variability, *Cont. Shelf Res.*, *11*(2), 123–137.
- Mooers, C. N. K., J. Fernandez-Partagas, and J. F. Price (1976), Meteorological forcing fields of the New York Bight (first year's progress report), technical report, Univ. of Miami, Coral Gables, Fla.
- Mountain, D. G. (2003), Variability in the properties of shelf water in the Middle Atlantic Bight, 1977–1999, *J. Geophys. Res.*, *108*(C1), 3014, doi:10.1029/2001JC001044.
- Nelson, W. R., M. C. Ingham, and W. E. Schaaf (1977), Larval transport and year-class strength of Atlantic menhaden. Brevoortia tyrannus, *U.S. Natl. Mar. Fish. Serv. Fish. Bull.*, *75*, 23–41.
- Ohlmann, C., P. White, L. Washburn, E. J. Terrill, B. Emery, and M. P. Otero (2007), Interpretation of coastal HF radar-derived surface currents with high-resolution drifter data, *J. Atmos. Oceanic Technol.*, *24*, 666–680, doi:10.1175/JTECH1998.1.
- Pawlowicz, R., R. C. Beardsley, and S. J. Lentz (2002), Classical tidal harmonic analysis including error estimates in MATLAB using T\_TIDE, *Comput. Geosci.*, *28*, 929–937.
- Perlin, A., J. N. Moum, and J. M. Klymak (2005), Response of the bottom boundary layer over a sloping shelf to variations in alongshore wind, *J. Geophys. Res.*, *110*, C10S09, doi:10.1029/2004JC002500.
- Quinlan, J. A., B. O. Blanton, T. J. Miller, and F. E. Werner (1999), From spawning grounds to the estuary: Using linked individual-based and hydrodynamic models to interpret patterns and processes in the oceanic phase of Atlantic menhaden Brevoortia tyrannus life history, *Fish. Oceanogr.*, *8*, 224–246.
- Schofield, O., et al. (2008), The decadal view of the Mid-Atlantic Bight from the COOLroom: Is our coastal system changing?, *Oceanography*, *23*(4), 108–117.
- Song, T., D. B. Haidvogel, and S. M. Glenn (2001), Effects of topographic variability on the formation of upwelling centers off New Jersey: A theoretical model, *J. Geophys. Res.*, *106*(C5), 9223–9240.
- Stewart, R. H., and J. W. Joy (1974), HF radio measurements of surface currents, *Deep Sea Res. Part I*, *21*, 1039–1049.
- Tang, D., et al. (2009), Shallow Water '06—A joint acoustic propagation/nonlinear internal wave physics experiment, *Oceanography*, *20*(4), 156–167.
- Teague, C. C. (1971), High frequency resonant scattering techniques for the observation of directional ocean-wave spectra, Ph.D. thesis, Stanford Univ., Palo Alto, Calif.
- Thieler, E. R., B. Butman, W. C. Schwab, M. A. Allison, N. W. Driscoll, J. P. Donnelly, and E. Uchupi (2007), A catastrophic meltwater flood event and the formation of the Hudson Shelf Valley, *Palaeogeogr. Palaeoclim. Palaeoecol.*, *246*(1), 120–136, doi:10.1016/j.palaeo.2006.10.030.
- Tilburg, C. E. (2003), Across-shelf transport on a continental shelf: Do across-shelf winds matter?, *J. Phys. Oceanogr.*, *33*(12), 2675–2688.
- Trowbridge, J., and S. Lentz (1991), Asymmetric behavior of an oceanic boundary layer above a sloping bottom, *J. Phys. Oceanogr.*, *21*(8), 1171–1185.
- Ullman, D. S., J. O'Donnell, J. Kohut, T. Fake, and A. Allen (2006), Trajectory prediction using HF radar surface currents: Monte Carlo simulations of prediction uncertainties, *J. Geophys. Res.*, *111*, C12005, doi:10.1029/2006JC003715.
- Werner, F. E., J. A. Quinlan, B. O. Blanton, and R. A. Luetlich (1997), The role of hydrodynamics in explaining variability in fish populations, *J. Sea Res.*, *37*(3–4), 195–212, doi:10.1016/S1385-1101(97)00024-5.
- Whitney, M. M., and R. W. Garvine (2005), Wind influence on a coastal buoyant outflow, *J. Geophys. Res.*, *110*, C03014, doi:10.1029/2003JC002261.
- Winant, C. D. (1980), Coastal circulation and wind-induced currents, *Annu. Rev. Fluid Mech.*, *12*(1), 271–301, doi:10.1146/annurev.fl.12.010180.001415.

- Yankovsky, A. E., and R. W. Garvine (1998), Subinertial dynamics on the inner New Jersey Shelf during the upwelling season, *J. Phys. Oceanogr.*, *28*(12), 2444–2458.
- Yankovsky, A. E., R. W. Garvine, and A. Münchow (2000), Mesoscale currents on the inner New Jersey Shelf driven by the interaction of buoyancy and wind forcing, *J. Phys. Oceanogr.*, *30*(9), 2214–2230.
- Yoder, J. A., S. E. Schollaert, and J. E. O'Reilly (2002), Climatological phytoplankton chlorophyll and sea surface temperature patterns in continental shelf and slope waters off the northeast US coast, *Limnol. Oceanogr.*, *47*(3), 672–682.
- Zhang, W. G., J. L. Wilkin, and R. J. Chant (2009), Modeling the pathways and mean dynamics of river plume dispersal in the New York Bight, *J. Phys. Oceanogr.*, *39*, 1167–1183.
- 
- S. M. Glenn, D. Gong, and J. T. Kohut, Institute of Marine and Coastal Sciences, Rutgers-State University of New Jersey, 71 Dudley Rd., New Brunswick, NJ 08901, USA. (glenn@marine.rutgers.edu; donglai@marine.rutgers.edu; kohut@marine.rutgers.edu)